



# Development, Phenotypic Characterization and Genomic Analysis of a *Francisella tularensis* Panel for Tularemia Vaccine Testing

Beth A. Bachert<sup>1†</sup>, Joshua B. Richardson<sup>2†</sup>, Kevin D. Mlynek<sup>1</sup>, Christopher P. Klimko<sup>1</sup>, Ronald G. Toothman<sup>1</sup>, David P. Fetterer<sup>3</sup>, Andrea E. Luquette<sup>4</sup>, Kitty Chase<sup>4</sup>, Jessica L. Storrs<sup>4</sup>, Ashley K. Rogers<sup>4</sup>, Christopher K. Cote<sup>1</sup>, David A. Rozak<sup>4</sup> and Joel A. Bozue<sup>1\*</sup>

## OPEN ACCESS

### Edited by:

Miklos Fuzi,  
Semmelweis University, Hungary

### Reviewed by:

Monique L. Van Hoek,  
George Mason University,  
United States  
Jieh-Juen Yu,  
University of Texas at San Antonio,  
United States

### \*Correspondence:

Joel A. Bozue  
joel.a.bozue.civ@mail.mil

† These authors have contributed  
equally to this work

### Specialty section:

This article was submitted to  
Infectious Diseases,  
a section of the journal  
Frontiers in Microbiology

**Received:** 15 June 2021

**Accepted:** 21 July 2021

**Published:** 11 August 2021

### Citation:

Bachert BA, Richardson JB,  
Mlynek KD, Klimko CP, Toothman RG,  
Fetterer DP, Luquette AE, Chase K,  
Storrs JL, Rogers AK, Cote CK,  
Rozak DA and Bozue JA (2021)  
Development, Phenotypic  
Characterization and Genomic  
Analysis of a *Francisella tularensis*  
Panel for Tularemia Vaccine Testing.  
*Front. Microbiol.* 12:725776.  
doi: 10.3389/fmicb.2021.725776

<sup>1</sup> Division of Bacteriology, United States Army Medical Research Institute of Infectious Diseases, Frederick, MD, United States, <sup>2</sup> Center for Genome Sciences, United States Army Medical Research Institute of Infectious Diseases, Frederick, MD, United States, <sup>3</sup> Division of Biostatistics, United States Army Medical Research Institute of Infectious Diseases, Frederick, MD, United States, <sup>4</sup> Biodefense Reference Material Repository, United States Army Medical Research Institute of Infectious Diseases, Frederick, MD, United States

*Francisella tularensis* is one of several biothreat agents for which a licensed vaccine is needed to protect against this pathogen. To aid in the development of a vaccine protective against pneumonic tularemia, we generated and characterized a panel of *F. tularensis* isolates that can be used as challenge strains to assess vaccine efficacy. Our panel consists of both historical and contemporary isolates derived from clinical and environmental sources, including human, tick, and rabbit isolates. Whole genome sequencing was performed to assess the genetic diversity in comparison to the reference genome *F. tularensis* Schu S4. Average nucleotide identity analysis showed >99% genomic similarity across the strains in our panel, and pan-genome analysis revealed a core genome of 1,707 genes, and an accessory genome of 233 genes. Three of the strains in our panel, FRAN254 (tick-derived), FRAN255 (a type B strain), and FRAN256 (a human isolate) exhibited variation from the other strains. Moreover, we identified several unique mutations within the *Francisella* Pathogenicity Island across multiple strains in our panel, revealing unexpected diversity in this region. Notably, FRAN031 (Schem) completely lacked the second pathogenicity island but retained virulence in mice. In contrast, FRAN037 (Coll) was attenuated in a murine pneumonic tularemia model and had mutations in *pdpB* and *iglA* which likely led to attenuation. All of the strains, except FRAN037, retained full virulence, indicating their effectiveness as challenge strains for future vaccine testing. Overall, we provide a well-characterized panel of virulent *F. tularensis* strains that can be utilized in ongoing efforts to develop an effective vaccine against pneumonic tularemia to ensure protection is achieved across a range *F. tularensis* strains.

**Keywords:** *Francisella tularensis*, vaccine, tularemia, *Francisella* pathogenicity island, virulence, mouse, animal modeling

## INTRODUCTION

*Francisella tularensis* is a gram-negative bacterium that causes the potentially life threatening and debilitating disease tularemia. *F. tularensis* is able to infect a wide range of animal species, including humans. *F. tularensis* can be transmitted to humans through a number of routes, the most common being the bite of an infected insect or other arthropod vector (Jellison, 1950; Markowitz et al., 1985; Ellis et al., 2002; Goethert et al., 2004). Human illness can range from the ulceroglandular form (most common and naturally occurring form of the disease) to more serious pneumonic or typhoidal tularemia (Ellis et al., 2002). In pneumonic tularemia (of most concern for the biodefense community), infection progresses from the lungs to other organs, primarily the liver and spleen (Saslaw et al., 1961a; Evans et al., 1985; Dennis et al., 2001; Twenhafel et al., 2009; Fritz et al., 2014; Heine et al., 2016). The risk of infection is associated mainly with two subspecies, the more virulent *F. tularensis* subsp. *tularensis* (type A) and the less virulent *F. tularensis* subsp. *holarctica* (type B).

Until agreement of the Biological Weapons Convention, *F. tularensis* had been weaponized for the potential use by several countries (Dennis et al., 2001). Due to its high pathogenicity, low infectious dose, and demonstrable virulence after aerosolization, *F. tularensis* poses a serious potential threat and therefore is classified by the United States (U.S.) Department of Health and Human Services as a Tier 1 Select Agent (Saslaw et al., 1961a,b; Harris, 1992; Dennis et al., 2001). A medical countermeasure gap for the U.S. military and biodefense communities is the lack of a Food and Drug Administration (FDA) approved vaccine to prevent pneumonic tularemia.

A live vaccine strain (LVS) derived from a type B strain of *F. tularensis* was previously developed and used in the former Soviet Union (Eigelsbach and Downs, 1961; Tigertt, 1962). In the U.S., LVS has been administered as an Investigational New Drug status vaccine to at risk laboratory workers since it does provide some level of protection against respiratory challenge with *F. tularensis* in human volunteers (McCrum, 1961; Saslaw et al., 1961a). However, LVS is not an ideal vaccine and has disadvantages, including the potential for systemic side effects and lack of complete understanding of the basis of attenuation (McCrum, 1961; Saslaw et al., 1961a; Rohmer et al., 2006). In addition, obtaining approval for LVS is complicated by its unknown history, instability of colony morphology, and potential reversion to virulence.

Thus, new efforts are underway to derive better pneumonic tularemia vaccine candidates for biothreat concerns which could gain FDA approval. The incidence of pneumonic tularemia in the U.S. and worldwide is very low and geographically spread out which would not be conducive to conducting human clinical vaccine trials. Therefore, animal models would be needed to test the protective efficacy of future tularemia vaccines. Two models, which have been shown to be similar to pneumonic tularemia in humans, are the rat aerosol challenge model (Jemski, 1981; Ray et al., 2010; Hutt et al., 2017) and the non-human primate (specifically the cynomolgus macaque) aerosolized *F. tularensis* challenge model (Glynn et al., 2015; Guina et al., 2018).

Several prospective tularemia vaccine candidates are being pursued, including *F. holarctica* and *F. tularensis* Schu S4 attenuated variants containing deletions in *capB*, a putative capsule biosynthesis gene (Conlan et al., 2010; Jia et al., 2010, 2016), *purMCD*, involved in nutrient metabolism (Pechous et al., 2008), and *clpB*, a heat shock gene (Conlan et al., 2010; Golovliov et al., 2013). The vast majority of vaccine candidates for tularemia have only been assessed for protection against the Schu S4 isolate. However, infection with the prototypical Schu S4 strain may not represent infection with diverse *F. tularensis* strains. Twine et al. (2006) initially compared the virulence of Schu S4 (obtained from the *Francisella* Strain collection) against another type A isolate, FSC033, showing that Schu S4 was less virulent during intradermal and aerosol infection of mice (Twine et al., 2006). The type A isolates can be further divided into subpopulations A1a, A1b, and A2, using molecular typing methods. These subpopulations differ in their geographical associations and degrees of virulence. For example, type A1 isolates primarily occur in the central U.S. while the type A2 isolates are mostly found in the western U.S. (Farlow et al., 2005), and type A1b isolates have been identified to result in significantly higher mortality during human infections than any other subtype (Kugeler et al., 2009). A more recent study showed that Schu S4 (BEI # NR-643), designated as type A1a, actually exhibited decreased virulence in mice compared to other type A1a strains as well as type A1b and A2 isolates (Molins et al., 2014). However, genetic differences have been demonstrated between the source of isolates of Schu S4 leading to variation in virulence (Lovchik et al., 2021).

A successful tularemia vaccine needs to protect against a wide variety of *F. tularensis* strains, which may differ in geographic origin or virulence attributes. In order to facilitate the efficacy testing of new vaccines against pneumonic tularemia, we developed a well-characterized panel of *F. tularensis* strains currently derived from various regions of the U.S. This panel represents a variety of historical, clinical, and environmental isolates that we have characterized phenotypically and genotypically and will be essential in the development of medical countermeasures against pneumonic tularemia for future vaccine testing in the appropriate animal models.

## MATERIALS AND METHODS

### Bacterial Strains

All *F. tularensis* strains used in this study are listed in **Table 1**. Single-use cultures were prepared by inoculating enriched chocolate agar plates obtained from Remel™ with source material and incubating for 24 h at 35°C in 5% CO<sub>2</sub>. Bacterial growth was re-suspended in Trypticase Soy Broth (BBL™) with 12.5% glycerol and stored at -70°C until needed. Single use vials from each lot were randomly checked for purity by observing colony morphologies on chocolate agar after 24, 48, and 72 h at 35°C in 5% CO<sub>2</sub>. The randomly selected aliquots were also Gram-stained to confirm appropriate staining and morphology under a microscope. Where indicated, *F. tularensis* was grown in Chamberlain's Defined Medium (CDM) (Chamberlain, 1965)

or brain heart infusion (BHI) broth supplemented with 1% Isovitalex (Becton Dickinson). All isolates were prepared under International Organization for Standardization (ISO) 17025 and ISO 17034 standard and are being retained and distributed via the Biodefense Reference Material Repository for this and any vaccine, therapeutic, and diagnostic studies.

## Genome Sequencing

DNA was isolated using the QIAgen EZ1 platform. DNA for each strain was sequenced using either the PacBio Sequel, using version 2 SMRT cells and template prep kit, or the Illumina MiSeq, using the v3 600 cycle kit and Nextera Flex library prep kit. If only PacBio reads were available, reads were quality filtered (quality >0.7) and assembled using HGAP4 (Chin et al., 2013), with default assembly parameters, except the Aggressive option was set to “On.” Reads were assembled into two contigs, and manually joined in Geneious, if necessary. Illumina reads had adapters removed and were quality trimmed using Trimmomatic v.0.33 (Bolger et al., 2014). PacBio reads were corrected using the Illumina reads and the program FilTlong (Wick, 2020). PacBio and Illumina reads were *de novo* hybrid assembled using Spades (Bankevich et al., 2012) and Unicycler (Wick et al., 2017). If complete *de novo* assemblies were not generated by Spades and/or Unicycler, draft assemblies were merged using flye’s subassemblies setting (Kolmogorov et al., 2019), and manual adjustments and circularization was then done in Ugene (Okonechnikov et al., 2012) and Mauve (Darling et al., 2010). Reads were mapped back to the draft assembly with Minimap2 (Li, 2018), and errors were corrected using Pilon (Walker et al., 2014). Genbank accession numbers are included in **Table 1**.

## Pan-Genome Analysis

Assembled genomes were annotated using the PROKKA (Seemann, 2014) pipeline through the Galaxy platform (Afgan et al., 2018). Average Nucleotide Identity was calculated using the method of Goris (Goris et al., 2007), on the Enve-omics platform (Rodriguez-R and Konstantinidis, 2016). A pan-genome analysis was performed with ROARY (Page et al., 2015), using the ten strains in the *Francisella* panel and the reference strain Schu S4, and with paralog splitting disabled. Core genes were defined as genes present in all ten strains, while the shell and cloud genes were defined as genes present in two or more strains, and genes present in 1 strain, respectively. The shell and cloud genes constitute the accessory genome. Results were visualized using Phandango (Hadfield et al., 2017), and a principal component analysis of the presence absence table was performed in R (R. C. Team, 2020) using the micropan package (Snipen and Liland, 2015) and custom scripts. UpSet analysis was performed with the UpSetR package in R (Conway et al., 2017).

## Growth Curves

Growth assays were performed in BHI or CDM, as indicated. Assays were performed using an Infinite M200 Pro (Tecan) microplate reader in 96-well microtiter plates at 37°C with shaking. The OD<sub>600</sub> was measured every 60 min. For all assays, *F. tularensis* strains were grown for 24 h on a chocolate

agar plate and then resuspended in broth medium to an approximately equal OD<sub>600</sub> (0.025). All samples were performed in quadruplicate and included medium controls to confirm sterility and for use as blanks to calculate the absorbance of the cultures.

## LPS Analysis

Whole-cell extracts were collected for LPS analysis from plate grown *F. tularensis* strains. Cultures were prepared at approximately equal colony forming unit (CFU) concentrations in PBS, lysed in gel loading buffer solution, and boiled for at least 45 min and confirmed to be inactivated. Samples were fractionated on NuPage Novex 4–12% Bis-Tris gels. For western analysis, fractionated material was transferred onto a nitrocellulose membrane using an iBlot Gel Transfer Device. After transfer, the membranes were blocked with 1% skim milk in Tris Buffered Saline + Tween 20. Samples were blotted with mouse monoclonal anti-LPS antibody (F6070-02X; US Biological; Salem, MA, United States) or anti-capsule antibody (11B7; Apicella et al., 2010) at dilutions of 1:500. The loading control antibody used for all analyses was rabbit polyclonal anti-*Escherichia coli* GroEL (dilution of 1:2,000) (Enzo Life Sciences; Farmingdale, NY, United States). Bands were visualized using 3,3′,5,5′-Tetramethylbenzidine Membrane Peroxidase substrate (Kirkegaard & Perry Laboratories, Inc; Gaithersburg, MD, United States).

## Intracellular Growth Analysis

J774A.1 cells, a murine macrophage-like cell line obtained from the American Type Culture Collection (TIB-67<sup>TM</sup>), were seeded ( $\sim 2.5 \times 10^5$  cells/well) into 24-well plates and cultured 2 days (37°C, 5% CO<sub>2</sub>) at which time the cells had formed confluent monolayers. The cells were maintained in Dulbecco’s Modified Eagle’s medium containing 10% heat-inactivated fetal bovine serum (Corning 10-013-CV). For the intracellular assays, *F. tularensis* was suspended in phosphate buffered saline (PBS) from a 24 h plate, and then diluted 1:5 in tissue culture medium. The bacterial suspension was added to the macrophages in 200  $\mu$ l of medium to achieve a multiplicity of infection (MOI) of  $\sim 100:1$ , and the MOI was confirmed from this suspension by serial dilutions and plating on chocolate agar plates. The bacteria and macrophages were allowed to co-incubate for 2 h at 37°C with 5% CO<sub>2</sub>. Next, the medium containing the extracellular bacteria was aspirated and replaced with fresh tissue culture medium supplemented with 25  $\mu$ g/ml of gentamycin for an additional 2 h. After this incubation, samples from the tissue culture wells were washed three times with PBS. The monolayer was then lysed with 200  $\mu$ l of sterile water, immediately scraped, and suspended in 800  $\mu$ l of PBS. The suspension was serially diluted in PBS and plated onto chocolate agar plates. The remaining tissue culture wells were assayed for CFU recovery at the 24 h post-infection time point as described above.

## Mouse Challenges

Virulence of each of the *F. tularensis* strains was assessed in BALB/c mice (7–9 week-old obtained from Charles River Laboratories) by intranasal challenge as previously described

(Bachert et al., 2019; Biot et al., 2020). Briefly, the titer of the challenge doses were determined by serial dilutions in PBS and plating on chocolate agar. Mice were anesthetized with 150  $\mu$ l of ketamine, acepromazine, and xylazine injected intraperitoneally. The mice were then challenged by intranasal instillation with 50  $\mu$ l from serial dilutions of *F. tularensis* suspended in PBS to an OD<sub>600</sub> of approximately 0.5 from freshly swabbed plate cultures grown for 24 h. Mice were monitored several times each day for 14 days for clinical signs, and mortality rates were recorded. Humane endpoints were used, and mice were euthanized when moribund according to an endpoint score sheet.

## Statistics

Growth analysis of bacterial strains in broth media was analyzed as previously described (Zweitering et al., 1990). A logistic growth equation was used to fit the data as a function of maximum density. For mouse challenge experiments, LD<sub>50</sub> values were determined under a probit model and median time to death or euthanasia (TTD) was estimated by the Kaplan–Meier method. Comparisons of the median TTD between strains are obtained from a log-normal accelerated failure time model of the form  $\text{Log}(\text{TTD}) = m \cdot \text{Log}(\text{Dose}) + b$ , where  $m$  and  $b$  are strain-specific slope and intercept terms. A Wald test was used to compare the model estimated median TTD at the middle of the dose curve. Analysis was implemented in PROC LIFEREG and PROC PROBIT, SAS version 9.4 (SAS Institute Inc., Cary, NC, United States).

## RESULTS

### Strain Collection

The Department of Defense's Biodefense Reference Material Repository (BRMR), which is housed at the United States Army Medical Research Institute for Infectious Diseases (USAMRIID), contains distinct *F. tularensis* isolates, which were obtained from historical and contemporary environmental and clinical sources and prepared according to ISO standards and guidelines for biological reference materials. These isolates were down-selected to the 10 potential candidate strains that were used in this study (Table 1) by loosely following guidelines laid out by Van Zandt et al. (2012) to support the creation

of a similarly motivated *Burkholderia* challenge panel. Most importantly, we preferentially selected strains that were known or believed to be close to the environmental or clinical source and were accompanied by clinical or laboratory evidence of virulence in humans or mammals. These strains can be broadly separated into historic and contemporary representatives of the pathogenic bacterium.

Three of the 10 strains in our panel (FRAN031/Scherm, FRAN037/Coll, and FRAN249/Schu S4) were derived from lyophilized samples (see Table 1), not long after being isolated from human patients in 1944, 1945, and 1941, respectively. The strains were isolated from human ulcers and a digital lesion (Hesselbrock and Foshay, 1945; Buchele and Downs, 1949; Eigelsbach et al., 1951). These isolates were the subject of early virulence studies in mice (Downs and Woodward, 1949) and embryonated eggs (Downs et al., 1947a), which showed that they were among the more virulent *F. tularensis* isolates.

Six of the strains used in this study (FRAN250-FRAN251 and FRAN253-FRAN256) had been isolated from clinical and environmental samples collected in the central U.S. during the past 5 years and donated to the BRMR by the Minnesota Department of Health (MDH). Four of the MDH strains came from human clinical samples, one was propagated from a rabbit spleen, and the sixth was extracted from a tick (Table 1). We deliberately included a type B strain, which had been derived from a human tissue sample, to ensure that both of the major *F. tularensis* subtypes were included in our panel. Molecular subtyping based on SNPs as described previously (Pandya et al., 2009), showed all of the remaining MDH strains were type A1a, except for FRAN256, which was type A2. Each of the MDH-supplied strains had undergone limited laboratory manipulation before being accessioned into the BRMR and used in this study. The MDH strains had not been tested in animal virulence studies prior to now.

The remaining two isolates used for this study, FRAN244 and FRAN249, are both versions of the commonly used Schu S4 strain. FRAN244 was prepared from the BEI Resources Schu S4 isolate (NR-10492), which is commonly used in *F. tularensis* studies. We selected this widely studied Schu S4 isolate, despite its uncertain propagation history, to compare to FRAN249, which we had propagated directly from a 1958 lyophilized sample. Since Schu S4 was originally propagated from a single colony pick in

**TABLE 1** | *Francisella tularensis* strains used in this study.

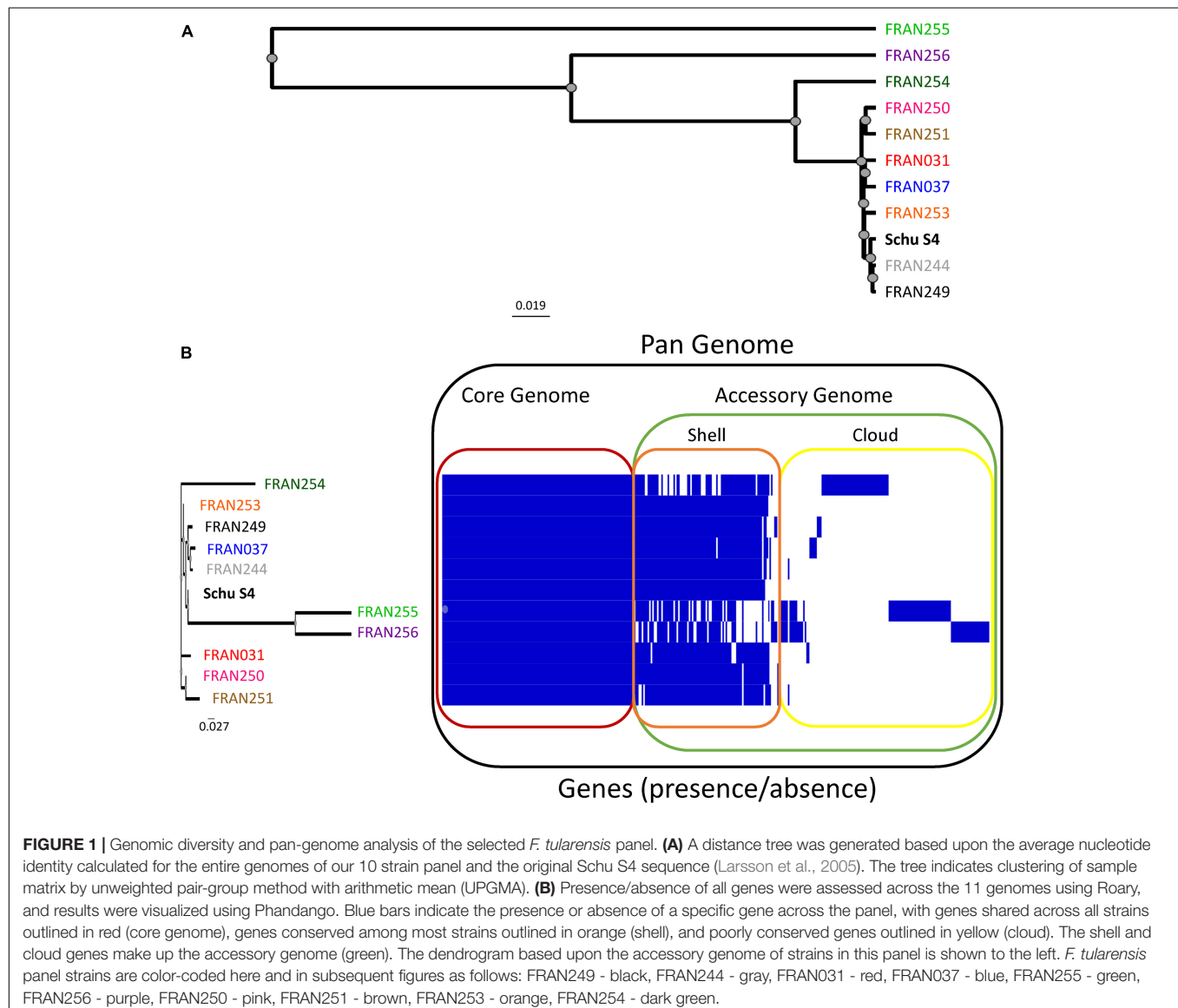
Strain	BRMR#	Type	Clinical description	GenBank #	Source/Reference
Schu S4	FRAN249	A1	Human ulcer, OH, 1941	CP073129	1958 USAMRIID Repository (Eigelsbach et al., 1951)
Schu S4	FRAN244	A1	Human ulcer, OH, 1941	CP073128	BEI Resources (NR-10492) (Eigelsbach et al., 1951)
Scherm	FRAN031	A1	Human, digital lesion, OH, 1944	CP073127	1954 USAMRIID Repository (Downs et al., 1947a)
Coll	FRAN037	A1	Human, digital ulcer, OH, 1945	CP073126	1948 USAMRIID Repository (Downs et al., 1947a)
2015321842	FRAN255	B	Human, male, pleura, KY, 2015	CP073125	MDH
2015315990	FRAN256	A2	Human, male, CSF, MT, 2015	CP073124	MDH
2014313438	FRAN250	A1a	Human, male bronchoalveolar lavage, IL 2014	CP073123	MDH
2017317779	FRAN251	A1a	Human, male, lung tissue, MN, 2017	CP073122	MDH
2016320786	FRAN253	A1a	Rabbit, male, spleen, MN, 2016	CP073121	MDH
2017314593	FRAN254	A1a	Tick, female, MN, 2017	CP073120	MDH

1951 (Eigelsbach et al., 1951), the lyophilized sample would have been no more than 7 years removed from the original isolate. It is worth noting that the 1958 sample, from which FRAN249 was derived, had a subpopulation with the *corC* gene containing a frameshift mutation. The *corC* gene had been previously shown to be involved in polyamine responsiveness and have a role in virulence (Russo et al., 2011). For this study, FRAN249 was propagated from a single colony pick that did not contain the *corC* mutation.

## Genomic Diversity and Pan-Genome Analysis of *F. tularensis* Panel

Whole genome sequencing was performed to assess the genetic diversity of the *F. tularensis* panel. To provide a measure of nucleotide level diversity across the panel for the entire genome, we calculated the pairwise Average Nucleotide Identity

(ANI), and constructed a distance tree based on this analysis (Figure 1A). On average, strains in the panel differ by approximately 0.001954%, translating to an average of 3,551 nucleotide differences between strains. The number of pairwise differences ranges from 23 (for closely related FRAN244 and FRAN249 strains) to 13,401 (for distantly related FRAN254 and FRAN255 strains). Supplementary Figure 1 shows the distance matrix for all strains. The level of diversity observed in this panel is typical of *F. tularensis*, as described previously and discussed further below (Vogler et al., 2009). In addition, we constructed a phylogeny of *F. tularensis* subsp. *holarctica*, *tularensis*, and *mediasiatica* strains that have complete genomes, including the newly sequenced strains in our panel, indicated in blue (Supplementary Figure 2). The tree is based on 100 conserved genes found within each strain. The genomes fall within three main clades corresponding to *holarctica*, *tularensis* type A2 and *tularensis* type A1. Within clade A1, the panel strains,

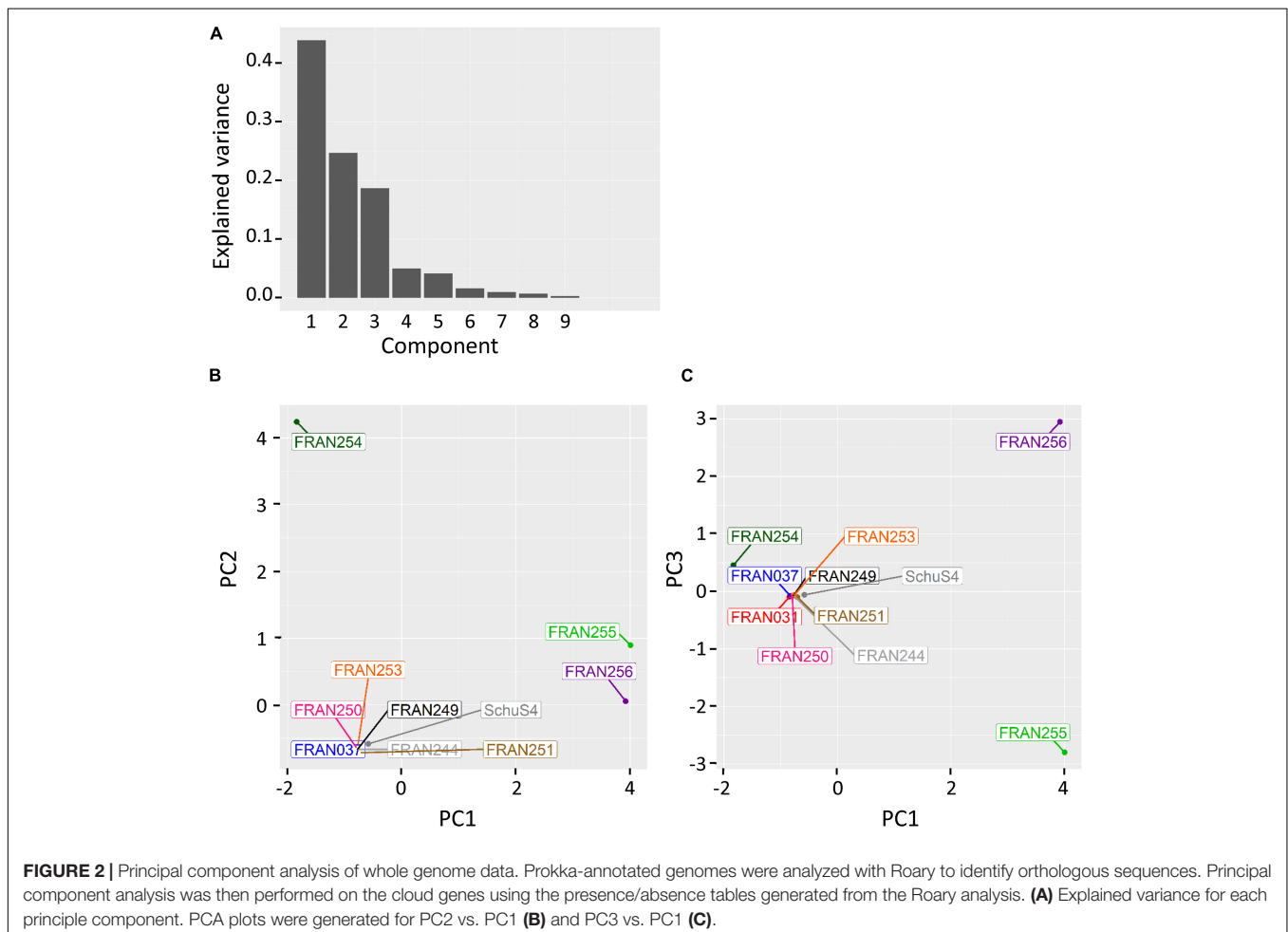


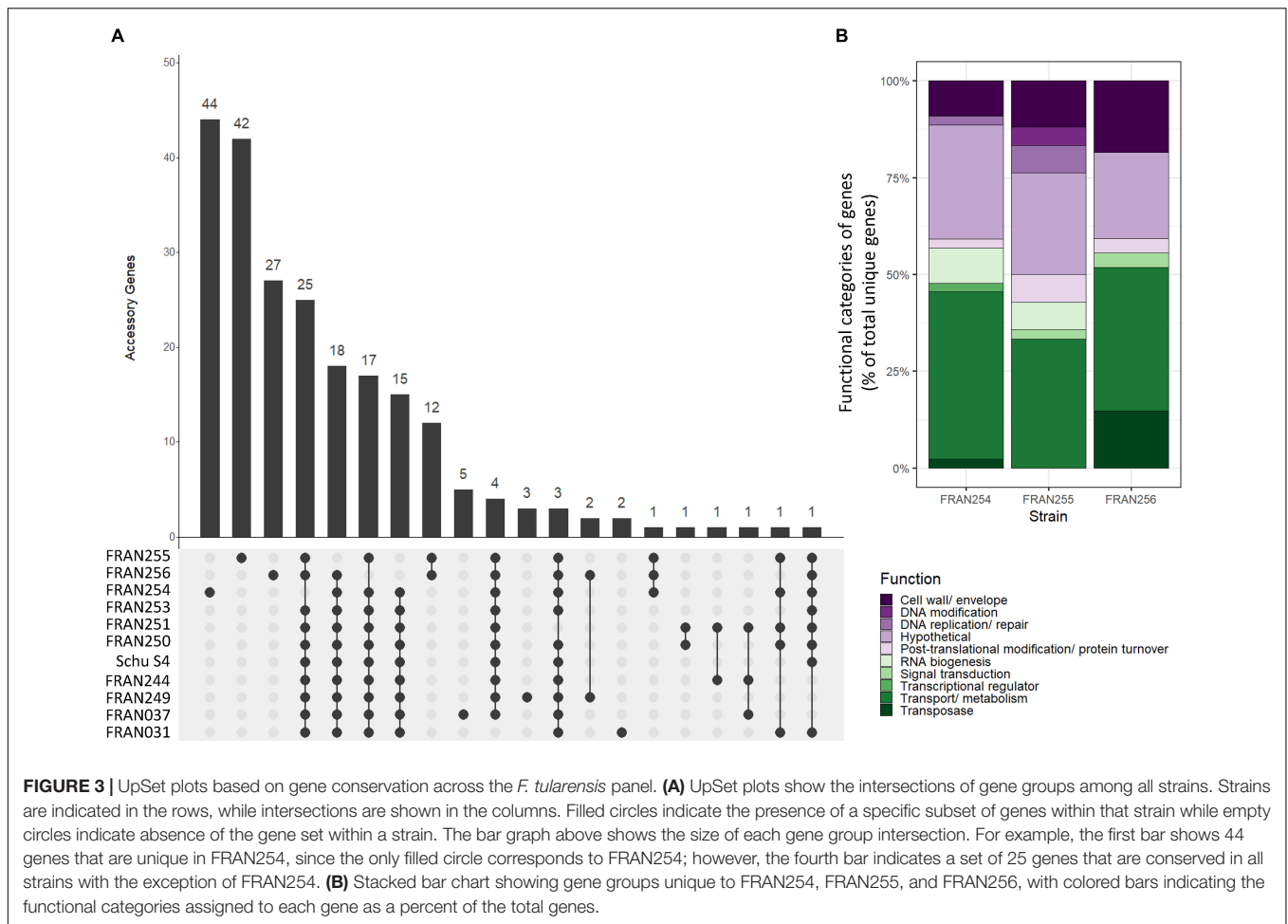
indicated in blue, occur throughout the clade, suggesting we have captured a reasonable amount of diversity. The tree also indicates low diversity in general within the type A1 clade, similar to what we observe in our nucleotide identity analysis.

We next performed a pan-genome analysis, in order to determine the number of “core” or conserved/essential genes as compared to the unique or “accessory” genes across these strains. **Figure 1B** shows the pan-genome of all 10 strains of the panel and the original Schu S4 genetic sequence (Larsson et al., 2005). The core genome, defined as genes present in all strains at >95% similarity at the amino acid level, consisted of 1,707 genes (red outline). The accessory genome, outlined in green, contains the shell and core genes that are conserved at various frequencies across the panel. One-hundred and seven genes were identified in the shell genome (orange outline), conserved in two or more strains, and 126 genes were identified in the cloud genome (yellow outline), present in 1 strain. The full list of each gene in the pan-genome, along with locus tags, are listed in **Supplementary Datasheet 1**. A dendrogram based upon the differences in presence/absence of genes in the accessory genome is shown in **Figure 1B** (left panel), and mirrors the pattern observed in **Figure 1A**, generated from the whole genome. FRAN255 and FRAN256 cluster separately from the other strains,

harboring more genes that are either unique or mutated, as compared to the rest of the panel. Similarly, FRAN254, the only tick isolate in our panel, clusters separately and contains a distinct pattern of unique genes (discussed below).

In order to further assess the genomic diversity of the strains in our panel, we performed principal component analysis (PCA) using the micropan package in R. **Figure 2** shows PCA plots based on cloud genes presence/absence identified by the Roary analysis. Principal components 1, 2, and 3 accounted for approximately 45, 25, and 20% of the variances across the *F. tularensis* panel, respectively (**Figure 2A**). PCA plots of our *F. tularensis* panel and the originally sequenced Schu S4 showed eight of the strains formed a single cluster, while the three remaining strains, FRAN254, FRAN255, and FRAN256, were isolated from the rest of the strains and from each other (**Figures 2B,C**). Both FRAN254 and FRAN256 are type A isolates derived from tick and male cerebrospinal fluid, respectively, while FRAN255 is a type B isolate from a male pleural sample. Collectively, the ANI, pan-genome, and PCA analyses demonstrate that the majority of the strains in our panel, including Schu S4 and its variants, have high genetic similarity, while FRAN254, FRAN255, and FRAN256 are more distant from these strains and from each other.





### Analysis of Mutated Genes Found in the *F. tularensis* Panel

To better understand the genetic changes driving the variation seen in the pan-genome analysis, UpSet plots were generated based on the accessory genome content of the panel strains. In the UpSet plot shown in **Figure 3**, strains are indicated in rows and the matrix (gray shaded region) shows the intersections, with filled circles indicating a set of genes is present in that strain, and empty circles indicating the set of genes is absent in that strain. Gene presence is defined as having greater than 95% similarity at the protein level. The corresponding bar graph shows how large these intersections are, i.e., how many genes are shared across this specific set of strains. The first 20 intersections representing the accessory genome are shown in **Figure 3**; the 1,707 genes within the core genome are not shown. A large number of these intersections encompass gene sets that were either unique in the FRAN254/255/256 trio or absent in these strains compared to the other *F. tularensis* strains (**Figure 3**). Notably, FRAN254, FRAN255, and FRAN256, which showed the most variation in the PCA analysis, had the highest number of unique gene sets, 44, 42, and 27, respectively. Twelve additional genes were shared by FRAN255 and FRAN256, while one gene, encoding a glycosyltransferase, was shared between all three strains. A total

**TABLE 2 |** Frequency of mutations and their functional categories in FRAN254, FRAN255, and FRAN256.

Functional category*	FRAN254		FRAN255		FRAN256		Total	
	No.	%	No.	%	No.	%	No.	%
Cell wall	4	9.1	5	11.9	5	18.5	14	12.4
DNA	1	2.3	5	11.9	0	0.0	6	5.3
PTM	1	2.3	3	7.1	3	11.1	7	6.2
RNA biogenesis	4	9.1	3	7.1	0	0.0	7	6.2
Regulation	1	2.3	1	2.4	1	3.7	3	2.7
Transport	19	43.2	15	35.7	10	37.0	44	38.9
Transposase	1	2.3	0	0.0	2	7.4	4	3.5
Hypothetical	13	29.5	10	23.8	6	22.2	28	24.8
Total	44	100.0	42	100.0	27	100.0	113	100.0

\*Mutated genes were assigned to one of the following functional categories: cell wall, DNA replication/repair (DNA), post-translational modification (PTM), RNA biogenesis, regulation, transport, transposase, or hypothetical. Number (No.) and frequency (%) of each functional category within strains or in total gene number are shown.

of 74 genes were absent in one or more of the trio in comparison to the rest of the panel. The remaining intersections contained 1–5 genes in each group that varied across the strains in our panel.

**TABLE 3** | Mutations identified in the *Francisella* pathogenicity islands.

	FPI-1					FPI-2					
	* <i>pdpA1</i>	* <i>pdpB1</i>	* <i>iglF1</i>	<i>pdpC1</i>	<i>pdpD1</i>	<i>anmK</i>	<i>pdpC2</i>	* <i>iglA2</i>	<i>pdpD2</i>	<i>anmK2</i>	<i>anmK1</i>
FRAN249	1401insA								495insT		
FRAN244			1647delT	2045delA							
FRAN031	Absent	Absent	Absent	Absent	Absent	Absent					
FRAN037		144delA; 966delA					232delA	1-129del			
FRAN256					198delA; 653delA; 1060delA	Fusion				1-246ins	591insA
FRAN251			1647delT	2045delA			2037delA				

\*Genes required for type VI secretion.

Data from our UpSet plot showed a large number of genes that are mutated in the FRAN254, FRAN255, and FRAN256 strains compared to the rest of our panel. We next aimed to characterize the function of these genes and the types of mutations present. BLAST search and multiple sequence alignments were carried out for each individual gene, and functional categories were assigned to each gene. **Table 2** shows the frequency of mutations identified in these strains and the functions of the genes in which these mutations were found. Of the 113 mutated genes, the vast majority fell into three categories: transport (38.9%), hypothetical (24.8%), and cell wall (12.4%). The inset in **Figure 3B** shows a stacked bar chart of these unique genes in FRAN254, FRAN255, and FRAN256, color-coded to indicate the percentage of genes belonging to each functional category. The percentage of genes in these categories were similar across all three isolates. Differences observed in FRAN254, FRAN255, and FRAN256 consisted of 70 insertions/deletions causing frameshifts, 19 in-frame insertions/deletions, 18 unique genes, 3 missense mutations, 2 gene duplications, and a single gene fusion. The complete list of genes and corresponding mutations are detailed in **Supplementary Datasheet 2**. Of note, FRAN256 harbored two transposases, ISFtu1 and ISFtu2, which differed in copy number as compared to the rest of the panel. 26 copies of ISFtu2 were observed in FRAN256, while this element was repeated up to 16 times in the remaining strains. ISFtu1, however, was duplicated only nine times in FRAN256 compared to 47 copies observed in most strains. Interestingly, we also observed several unexpected mutations within the *Francisella* Pathogenicity Island (FPI) of multiple strains within our panel, described below.

## Sequencing of the FPI Reveals Diverse Patterns of Mutations Across the *F. tularensis* Panel

Sequencing of our *F. tularensis* panel revealed diverse mutations across both FPI in several strains. These mutations occurred in the *pdpA*, *pdpB*, *iglF*, *pdpC*, and *pdpD* genes of the first FPI, and in the *pdpC*, *iglA*, and *pdpD* genes of the second FPI (**Table 3**). Notably, FRAN031 completely lacked the first FPI and had an intact copy of the second FPI with no notable mutations in any of the genes. All of the mutations, with the exception of an in-frame deletion in *iglA2*, were single base-pair insertions or deletions that resulted in a frameshift and premature

stop codon in each gene. A map of the mutations identified in FPI-1 and FPI-2 of the strains in our *F. tularensis* panel is shown in **Figure 4**. FRAN249 harbored mutations in *pdpA1* and *pdpD2*. Interestingly, FRAN244 and FRAN251 harbored identical mutations in *iglF1* and *pdpC1*, with FRAN251 containing an additional mutation in *pdpC2*. FRAN251 was the only strain in our panel harboring mutations in both copies of an FPI gene. FRAN037 contained frameshift mutations in *pdpB1* and *pdpC2*, and a unique in-frame deletion of the first 129 bp of the *iglA2* gene. Lastly, FRAN256 harbored multiple single bp deletions in *pdpD1*, presumably resulting in several truncated protein products, as well as unique *anmK* variants in both FPI regions. The *anmK* gene was represented by a single ORF in FPI-1, while *anmK1* was extended and *anmK2* was truncated in FPI-2. The diversity of FPI mutations within the *F. tularensis* panel was unexpected, although experiments described below suggest the majority of these mutations did not diminish the virulence of these strains, possibly because of the redundancy that exists between the duplicated FPIs.

## Growth of the *F. tularensis* Panel in BHI and CDM

For the 10 strains considered for the panel, growth of the strains was assayed on both solid agar medium and in two different types of broth media. For nine of the strains, no difference in colony size was noted. However, FRAN255 formed smaller colonies when compared to Schu S4 and required longer growth time (3 days versus 2 days) to form CFU that were countable (**Supplementary Figure 3**). Growth of the strains was also examined in broth media to include BHI with 1% Isovitalex (complex medium) (**Figure 5A**) and CDM (nutritionally defined medium) (**Figure 5B**). When grown in BHI, the two versions of Schu S4 (FRAN244 and FRAN249) grew to a maximum OD<sub>600</sub> of approximately 0.5 in agreement with our previous observations with Schu S4 (Kijek et al., 2019). In contrast, all of the other *F. tularensis* strains were never able to reach the OD<sub>600</sub> observed for Schu S4 (**Figure 5A**). FRAN256 exhibited a consistently lower OD<sub>600</sub>, although not statistically significant, while the remaining seven strains reached a maximal OD<sub>600</sub> that was significantly lower than that of Schu S4. However, when the strains were grown in CDM, a much higher OD<sub>600</sub> was reached for all strains. The only strain from this panel which was found to be significantly

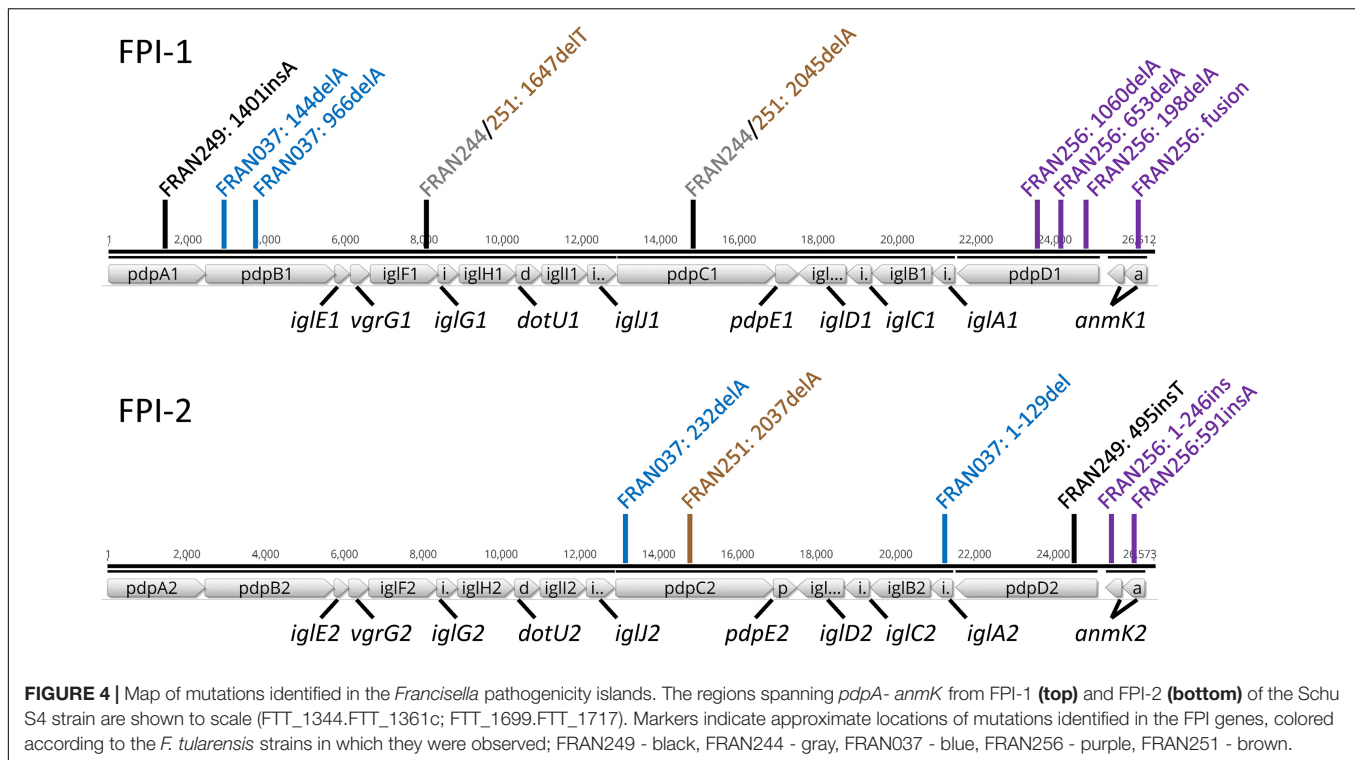


**FIGURE 4 |** Map of mutations identified in the *Francisella* pathogenicity islands. The regions spanning *pdpA*-*anmK* from FPI-1 (top) and FPI-2 (bottom) of the Schu S4 strain are shown to scale (FTT\_1344.FTT\_1361c; FTT\_1699.FTT\_1717). Markers indicate approximate locations of mutations identified in the FPI genes, colored according to the *F. tularensis* strains in which they were observed; FRAN249 - black, FRAN244 - gray, FRAN037 - blue, FRAN256 - purple, FRAN251 - brown.

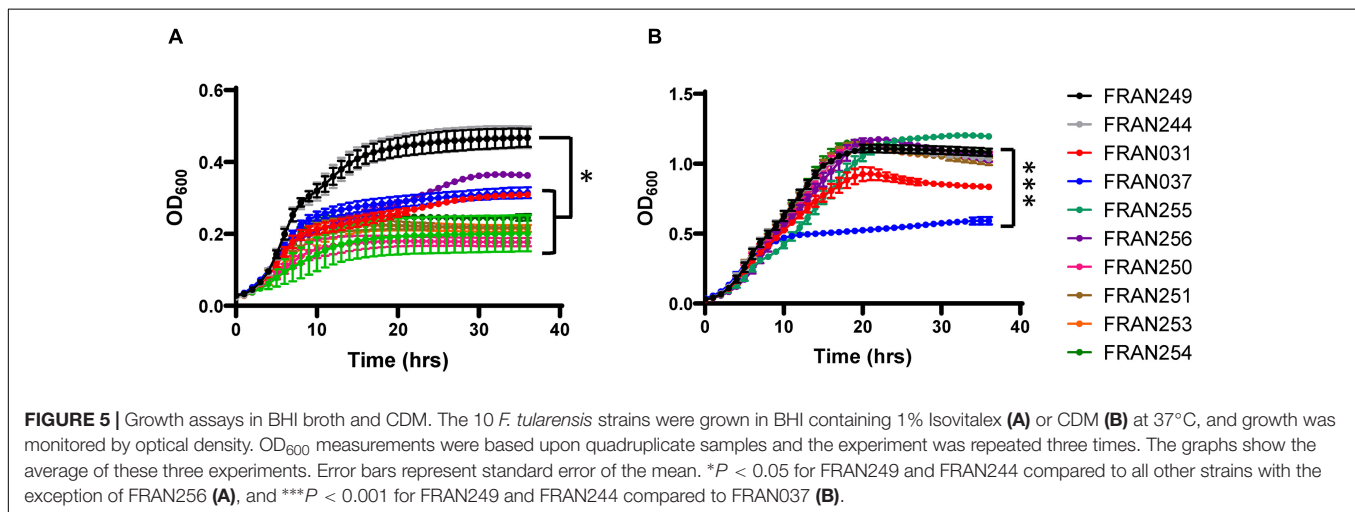


**FIGURE 5 |** Growth assays in BHI broth and CDM. The 10 *F. tularensis* strains were grown in BHI containing 1% Isovitalex (A) or CDM (B) at 37°C, and growth was monitored by optical density. OD<sub>600</sub> measurements were based upon quadruplicate samples and the experiment was repeated three times. The graphs show the average of these three experiments. Error bars represent standard error of the mean. \* $P < 0.05$  for FRAN249 and FRAN244 compared to all other strains with the exception of FRAN256 (A), and \*\*\* $P < 0.001$  for FRAN249 and FRAN244 compared to FRAN037 (B).

decreased in maximal OD<sub>600</sub> as compared to the Schu S4 strains was the FRAN037/Coll ( $P < 0.001$ ) (Figure 5B).

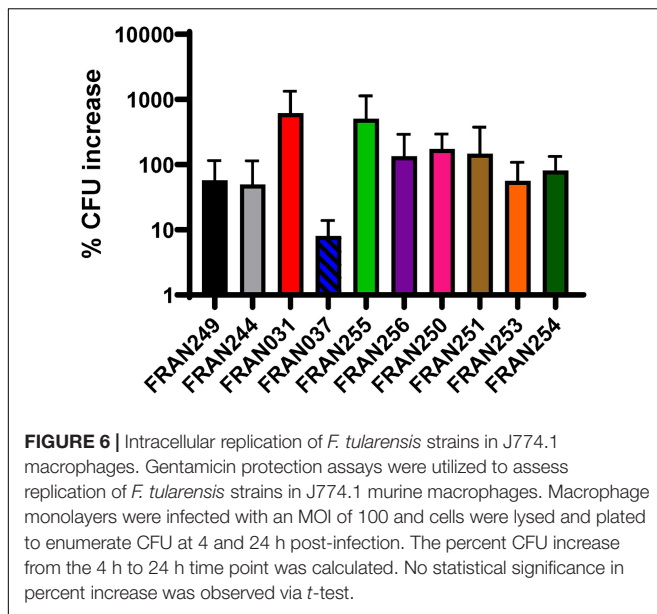
### *F. tularensis* Panel Strains Show Similar Levels of Intracellular Replication in Macrophages

As the ability to replicate within host cells is a hallmark of *F. tularensis* pathogenesis, we analyzed the ability of the 10 strains to grow intracellularly within J774 cells. As shown in Figure 6, all strains showed the ability to grow within the macrophage-like cells as the Schu S4 strains and increased in CFU numbers 2–3 logs, except for the FRAN037/Coll strain.

Although the replication defect was not statistically significant, the results with FRAN037 suggested that this historical strain could be attenuated.

### All *F. tularensis* Isolates, Except FRAN037, Exhibited Similar Virulence in Mice

To confirm the strains entered into the diversity panel were virulent, a pneumonic tularemia murine model was used. Though mice are not ideal for tularemia vaccine models, they are suitable for assessing *F. tularensis* virulence (Conlan et al., 2003; Chen et al., 2005; Fritz et al., 2014). Therefore, LD<sub>50</sub>



analysis was performed with all 10 strains by intranasal challenge of BALB/c mice (Figure 7 and Table 4). As expected for both versions of Schu S4 (FRAN244 and FRAN249), and in agreement with previous results from our laboratory and others (Chance et al., 2017), the LD<sub>50</sub> measurements for both versions were found to be <1 CFU.

Two additional historical *F. tularensis* strains considered for the panel were FRAN031 (Scherm) and FRAN037 (Coll). The mouse LD<sub>50</sub> values for these strains was originally reported as the dilution of a standard suspension which killed 50% of the mice by intraperitoneal challenge and assayed to be 10<sup>-9.2</sup> and 10<sup>-8.8</sup>, respectively (Downs et al., 1947b). To confirm the virulence of these historical strains and obtain the LD<sub>50</sub> with an actual CFU value, we tested these strains by intranasal challenge in this model. The LD<sub>50</sub> value for FRAN031 (Scherm) was also found to be <1 CFU. In contrast, no mice succumbed to challenge with the FRAN037 (Coll) strain at any of the challenged doses; thus, the LD<sub>50</sub> would be >2,080 CFU. Based upon the results described here, we will not be advancing FRAN037 (Coll) to be part of the diversity panel.

As no additional data were available for the clinical and environmental isolates obtained from the MDH other than listed in Table 1, we chose to confirm virulence in the mouse model prior to including these strains into the diversity panel. All proposed strains were found to be highly lethal in mice, and the LD<sub>50</sub> determined to be <1 CFU.

The only virulent *F. tularensis* strain that showed any significant difference in TTD across all tested challenge doses was FRAN255 when compared to the other lethal strains. The *P*-values when comparing TTD of FRAN255 to the other virulent strains was calculated to be as follows: FRAN249 (*P* = 0.0281), FRAN244 (*P* ≤ 0.0001), FRAN031 (*P* = 0.0008), FRAN250 (*P* ≤ 0.0001), FRAN251 (*P* = 0.0004), FRAN252 (*P* = 0.0005), FRAN253 (*P* = 0.0007), FRAN254 (*P* = 0.0051), and FRAN256 (*P* = 0.0001). However, as described above, FRAN255 also displayed a slower growth on agar plates compared to all the other

strains in our panel (Supplementary Figure 3) and in BHI broth when compared to most of the other strains (Figure 5A).

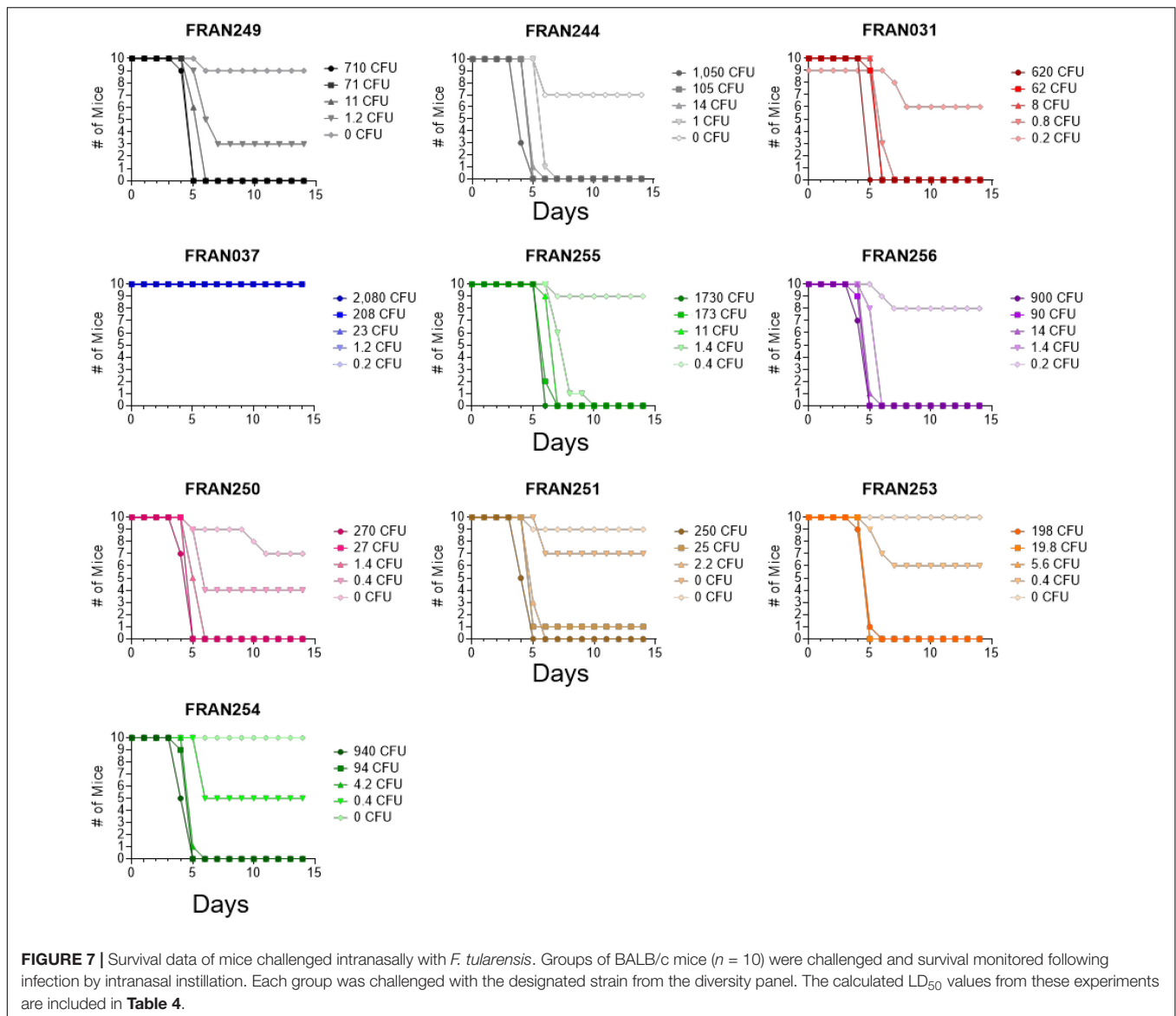
## Analysis of O-Antigen Profiles Across the *F. tularensis* Panel

One of the major virulence factors of *Francisella* is the lipopolysaccharide (LPS) and O-antigen capsule, which plays an important role in evasion of the host immune response (Sandstrom et al., 1992; Wang et al., 2006, 2007; Weiss et al., 2007; Kanistanon et al., 2008). In addition, mutations in *F. tularensis* LPS or capsule biosynthesis genes lead to attenuation (Raynaud et al., 2007; Apicella et al., 2010; Kim et al., 2012; Jones et al., 2014; Rasmussen et al., 2014, 2015; Chance et al., 2017). Therefore, we screened the O-antigen profile of our *F. tularensis* strains with monoclonal antibodies to both structures to determine if any differences were noted amongst the panel. As shown in Figure 8, when using an anti-LPS or anti-capsule monoclonal antibody for western gels, the overall banding pattern was similar for all 10 strains. A subtle difference was noted for FRAN255 in the staining intensity of the bands at the higher molecular weight region. However, the loading control for this study was anti-GroEL, and no differences in banding intensities were noted between any of the strains.

## DISCUSSION

### Need for a Tularemia Vaccine-Testing Panel

The lack of an FDA approved tularemia vaccine is a gap for the biodefense community. LVS has been utilized as an investigational vaccine since the 1960's. In addition, it does not provide full protection against aerosol exposure to *F. tularensis* and retains residual virulence (Eigelsbach and Downs, 1961; Tigertt, 1962). Vaccine candidates worthy of advanced development must be safer than LVS and provide comparable or greater protection against challenge with aerosolized *F. tularensis* Schu S4 (Jia and Horwitz, 2018). Significant efforts have been made toward vaccine development and characterization. Several live attenuated mutants of *F. tularensis* have been derived and tested for protective efficacy against Schu S4, including the Schu S4 deletion mutants  $\Delta clpB$ ,  $\Delta FTT0198/\Delta capB$  (Conlan et al., 2010) and *purMCD* (Pechous et al., 2008). A series of studies by Jia et al. (2010) assessed the efficacy of LVS  $\Delta capB$ , containing a deletion in the putative capsule biosynthesis gene, as well as LVS  $\Delta capB$  overexpressing the type VI secretion genes *iglA/B/C* (Jia et al., 2013, 2016, 2018). Another study has also shown that a *F. novicida iglD* mutant was able to protect both rats and NHPs against *F. tularensis* challenge (Chu et al., 2014). From both a safety and regulatory approval perspective, a subunit vaccine may be preferred to avoid the concerns of a live *Francisella* strain being used (Post et al., 2017; Mansour et al., 2018; Marshall et al., 2018; Whelan et al., 2018). However, live attenuated vaccine strains may provide better protection as they have the ability to establish a mild infection in the host, mimicking the infection of fully virulent strains and presenting appropriate antigens to the



immune system to induce durable antibody and cell-mediated immune responses (Drabner and Guzman, 2001).

Regardless of the type of vaccine, the majority of tularemia protection studies typically use the prototypical Schu S4 strain for challenge. However, differences in virulence exist between different laboratory stocks of Schu S4, as shown by a recent study that used a pneumonic tularemia model with both Fischer 344 rats and New Zealand white rabbits (Lovchik et al., 2021). Ideally, a common set of index *F. tularensis* strains would be used by the biodefense community for future vaccine and therapeutic countermeasure development research to protect against pneumonic tularemia. Therefore, we generated and characterized a panel of *F. tularensis* strains for the purpose of assessing future vaccine efficacy across a range of isolates in appropriate animal model, such as aerosol challenged Fisher rats and cynomolgus macaques. With this panel, a thorough genomic, *in vitro*, and *in vivo* characterization was performed with the 10 strains. The genomic analysis consisted of whole genome

sequencing using a mixture of long and short read technologies to generate complete, circularized genomes. Assembled genomes were subjected to ANI, phylogenetic and pan-genome analysis to measure the genetic variation present across the strain panel. Our *in vitro* characterization included growth curves, LPS profiles, and intracellular replication macrophage assays. We assessed initial virulence of the panel as measured by LD<sub>50</sub> determinations using an intranasal murine model of infection. However, as mice are extremely susceptible to *F. tularensis*, ongoing studies are currently assessing any virulence differences between the panel strains in the Fischer 344 rat aerosol challenge model (Jemski, 1981; Ray et al., 2010; Hutt et al., 2017).

## Genomic Diversity of the *F. tularensis* Panel

Whole genome sequencing of our *F. tularensis* panel revealed high genetic similarity within *F. tularensis* (>99% nucleotide

identity). We identified an average of 3,551 nucleotide differences among strains, with a range of 23 (closely related strains) to 13,401 (distantly related strains) differences. Further characterization of these strains by pan-genome analysis showed a total of 1,707 genes in the core genome. The accessory genome was found to contain 107 shell genes and 126 cloud genes that vary from strain to strain within the panel, and which could affect the responsiveness of these strains to vaccine treatments. A recent study characterized the pan-genome of 26 *Francisella* strains, and found the genus contained 4,053 genes, with a relatively small core genome of 692 genes (Kumar et al., 2020). However, this analysis was conducted on strains of differing species. To our knowledge, no pan-genome analysis has been conducted on strains of the same species of *F. tularensis*. Within-species variation is not well characterized in *F. tularensis*, though it is considered a clonal organism with highly conserved genomic sequence. A previous study reported an average nucleotide identity of  $\geq 99\%$  within subspecies of *F. tularensis* subsp. *holarctica* (Vogler et al., 2009), so the high level of genetic similarity in our study is not surprising. Strains in our panel are derived from a variety of hosts, geographical locations, and dates; therefore, the level of genomic variation we observe is representative of *F. tularensis*.

## Exclusion of FRAN031 and FRAN037 From the Vaccine-Testing Panel

Both the FRAN031 (Scherm) and FRAN037 (Coll) clinical isolate strains were described as being highly virulent (Downs et al., 1947a), and the genomic sequence for FRAN031 was previously reported in the literature (Pandya et al., 2009; Johnson et al., 2015). Based upon these previous studies, the absence of the FPI in FRAN031 and mutations in the FPI regions of FRAN037, which most likely lead to its attenuation, were unexpected observations in our current study. From the studies we have performed in a mouse model of infection, FRAN031 showed no virulence defect despite missing one of the pathogenicity islands (PAI) (Table 4). Granted, *F. novicida* also contains only one PAI and still highly virulent for mice (Biot et al., 2020).

FRAN037 was the only isolate in our panel that showed attenuation in both murine macrophages and intranasal mouse infection models. Several observations about the mutations identified in the FPI of FRAN037 may explain this attenuation. Firstly, FRAN037 harbored two unique frameshift mutations in the *pdpB1* gene. PdpB has been designated a homolog of IcmF, a known component of the type VI secretion system (T6SS). Multiple studies have demonstrated PdpB localizes to the inner membrane and is required for intracellular growth, supporting its role as a structural T6SS protein (Tempel et al., 2006; de Bruin et al., 2007, 2011; Schmerk et al., 2009b). Since PdpB1 is known to be a structural type VI secretion system protein, located on the inner membrane, a non-functional variant could potentially render the entire multi-subunit needle complex non-functional. Expression of a second mutated variant could be more deleterious to the cell than having a single functional variant. Additionally, FRAN037 contained an in-frame deletion of the first 42 amino acids of the IglA2 protein, also a unique mutation in our panel.

IglA is also a structural component of the T6SS, interacting with IglB to form the contractile sheath of the needle complex. We hypothesize that the mutations found in one or both of these structural proteins, IglA and PdpB, may lead to a dominant negative effect and cause the attenuation observed in FRAN037. As such, this strain will not be included as part of the diversity panel for further testing. Likewise, the lack of the FPI in FRAN031 was unexpected. Therefore, we will also not be including this strain as part of our formal panel strain for further testing.

The exact reasons for the occurrence of the FPI mutations identified in these historical strains remains to be determined. For the purpose of this study, we attempted to use isolates as close to the original isolate as available in the USAMRIID repository (Table 1). Based upon previous literature, Coll (FRAN037) should have been a fully virulent strain in mice (Downs and Woodward, 1949). However, in our tularemia intranasal challenge model in BALB/c mice, FRAN037 was completely attenuated at the doses used. The question remains if previous handling of this isolate prior to preparation for long-term storage lead to the mutations and attenuation or if these genetic mutations were already present from original 1945 isolate. Previous mouse virulence assays (Downs and Woodward, 1949) were performed by intraperitoneal challenge versus intranasal challenge as done here. In addition, it is unclear what mouse strain was used for these previous experiments. Perhaps these differences in the virulence characterization of FRAN037 could lead to these discrepancies in the mouse LD<sub>50</sub> studies and these genetic mutations in FRAN037 have always been present. The same questions remain for FRAN031 and loss of the FPI. We cannot rule out if the FPI was absent from the genome since its original isolation (1944) or this occurred at some point once prior to preparation for long term storage.

## Variation in the FPI Region

The 1958 version of Schu S4, FRAN249, harbored a frameshift mutation in the *pdpA1* gene, the first gene encoded by the FPI. Studies by Schmerk et al. (2009a,b) showed that *pdpA* of *F. novicida* was necessary for virulence in mice, replication in

TABLE 4 | Mouse intranasal LD<sub>50</sub> and TTD measurements.

Strain	Time to death (days)						
	LD <sub>50</sub> (CFU)	10 <sup>-2</sup> -10 <sup>-1</sup> CFU	10 <sup>-1</sup> -10 <sup>0</sup> CFU	10 <sup>0</sup> -10 <sup>1</sup> CFU	10 <sup>1</sup> -10 <sup>2</sup> CFU	10 <sup>2</sup> -10 <sup>3</sup> CFU	10 <sup>3</sup> -10 <sup>4</sup> CFU
FRAN249	<1	N/A	>14	6.5	6	5	5
FRAN244	<1	N/A	>14	6	5	5	4
FRAN031	<1	>14	6	6	6	5	N/A
FRAN037	>2,080	N/A	>14	>14	>14	>14	>14
FRAN255*	<1	N/A	>14	8	7	6	6
FRAN256	<1	N/A	>14	6	5	5	5
FRAN250	<1	>14	6	5.5	5	5	N/A
FRAN251	<1	>14	>14	5	5	4.5	N/A
FRAN253	<1	>14	>14	5	5	5	N/A
FRAN254	<1	>14	>14	5	5	4.5	N/A

\*Significantly higher TTD observed compared to other strains.

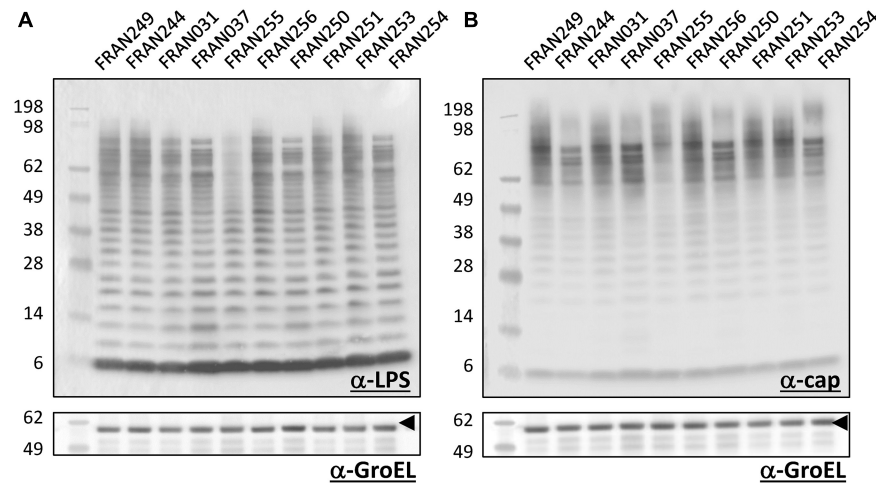


**FIGURE 8 |** Western blot analysis of *F. tularensis* strains. Pellets of the 10 *F. tularensis* strains were lysed. Extracts were run on SDS-PAGE gels at equal concentrations and blotted with either a monoclonal antibody to the O-antigen of LPS (A) or capsule (B) of *F. tularensis*. Equal loading of sample material was demonstrated when blotting the extracts with a polyclonal antibody directed against the GroEL protein (indicated by the arrowheads). Molecular masses are indicated on the left in kDa.

murine macrophages, and involved in interruption of host cell signaling. However, PdpA is not believed to be a structural component of the T6SS, since it bears no homology to structural T6SS proteins from other bacteria, and the exact biological role of PdpA is not well defined. In our study, FRAN249 showed no virulence difference in the mouse intranasal infection model; however, a functional *pdpA* copy is present on the second FPI which could compensate for a non-functional *pdpA*. Indeed, the function of many of the FPI proteins have been defined using *F. novicida*, which contains only a single FPI. Given that all of our strains, except FRAN037, retained virulence in the mouse model of intranasal infection, a simple explanation could be that a functional copy of the gene was supplied on the duplicated pathogenicity island.

Other mutations in the FPI have been previously reported in a comparative genomics study between the Schu S4 strain and WY96, representing type A1 and type A2 strains, respectively (Beckstrom-Sternberg et al., 2007). Of the 60 polymorphisms identified across both FPI regions, mutations resulting in premature stops occurred only in *pdpC*, *pdpD*, and several hypothetical proteins, while the *pdpA*, *pdpB*, and *iglABCD* genes remained intact (Beckstrom-Sternberg et al., 2007). Our study also identified frameshift mutations causing premature stops in *pdpC* and *pdpD*, indicating these genes are not as crucial for virulence. Our study identified additional mutations causing truncated variants of *pdpB1* and *iglA2*; however, they were only found in FRAN037, which was completely attenuated, whereas WY96 has been described as a virulent type A isolate. Notably, this study found no SNPs in *iglA* and determined *pdpB* to be under purifying selection, further supporting their importance in virulence and survival of *Francisella*. One unusual observation from our study was the presence of two identical mutations in FPI genes of two different panel strains, FRAN244 and FRAN251. Although these strains differ in geographical origin, clinical

source, and date of isolation (1941 vs. 2017), they contain the same mutations: 1647delT in *iglF1* and 2045delA in *pdpC1*.

Notably, FRAN251 is the only isolate in our panel that is presumed to contain two non-functional copies of an FPI gene. Both copies of *pdpC* contain a single bp deletion causing a frameshift and premature stop codon. A previous study assessed the effect of loss of *pdpC* in LVS on expression of the surrounding FPI genes and showed that membrane integrity was still maintained in the mutant, but it was unable to escape the phagosome and was significantly attenuated during intradermal infection of mice. Interestingly the *pdpC* LVS mutant exhibited a cytopathogenic response, due to its fragmentation of the phagosomal membrane and subsequent triggering of the inflammasome (Lindgren et al., 2013); this study noted that this is very different from the effect of an *iglC* mutant which does not show this hyper-cytotoxicity.

Interestingly, the *anmK* genes of FRAN256 differed from the rest of the panel within both FPI regions. It has been previously reported that *anmK* within *F. novicida* (also referred to as *pmcA*), encoding a 371 amino acid chaperone-like protein, is divided into two ORFs in Schu S4 (Nano and Schmerk, 2007). Similarly, all the type A isolates in our panel, with the exception of FRAN256, contained two ORFs, *anmK1* and *anmK2*. FRAN256 harbored a single ORF for *anmK* in FPI-1, while *anmK1* harbored a 246 bp insertion, and *anmK2* harbored a deletion causing a truncated variant. Type B strains were previously reported to contain a large deletion in the *anmK* and *pdpD* genes (Nano et al., 2004); however, FRAN255 harbored no such deletion and showed similar ORFs in this region as compared to the type A variants.

The presence of the observed SNPs within the FPIs of these strains was unexpected since this region encodes for proteins making up the Type VI secretion system and shown to be essential for virulence. The PAI is duplicated in all subspecies of *F. tularensis*, except for *F. novicida* (Nano et al., 2004;

Larsson et al., 2009). The exact role for the duplication of the PAI duplication remains to be determined. The G + C content of the FPI in contrast to the rest of the *Francisella* genome suggests it was acquired via horizontal gene transfer. Evidence suggests that the redundancy of the FPI compensates for the loss of some of the loci in this region (Bröms et al., 2010). The results of our current study would support this idea as we found SNPs in the FPI of five of the panel strains, but they retained full virulence in the pneumonic murine tularemia model. The exception to this is the FRAN037/Coll strain in which mutations occurred in genes encoding for structural proteins, *pdpB* and *iglA*. However, a previous study suggests (at least for LVS) both copies of *iglABCD* are necessary for optimal virulence in mice (Su et al., 2007).

### Variation in Other Genes of Interest

The UpSet plot analysis of the *F. tularensis* panel showed a large number of unique genes within the FRAN254, FRAN255, and FRAN256 strains as compared to the rest of the panel. Two of these genes corresponded to IS5 family transposase elements, ISFtu1 and ISFtu2, which were duplicated at differing frequencies across strains. Interestingly, the FRAN256 genome contained 26 copies of this mobile element while other panel strains contained up to 16 copies. These copies occurred in the same locations as those identified in the Schu S4 strain, with the exception that many of those elements were duplicated at those loci in the FRAN256 strain. Conversely, we observed that a second mobile element, ISFtu1, lacked additional copies in FRAN256 that were observed in other strains. This element was repeated 46–51 times in the genome of our panel strains, but only occurred nine times in FRAN256. Transposase activity often leads to genome rearrangements and gene deletions in bacteria, and it has been proposed that expansion of IS elements occurs as free-living bacteria transition to an intracellular lifestyle, where many of the genes are non-essential in the nutrient-rich host environment (Moran and Plague, 2004). The difference in IS element copy number in FRAN256 could indicate this strain is at a different evolutionary stage than the other strains included in our panel.

In our UpSet plot, a single gene group was found to be shared between FRAN254, FRAN255, and FRAN256. Further investigation revealed three copies of this gene in the *Francisella* genome, and that the encoded protein harbors a glycosyltransferase domain containing a DXD motif (PFAM04488). Interestingly, FRAN254, FRAN255, and FRAN256 harbor one functional copy of this gene, and two copies containing frameshift mutations. In the *F. tularensis* Schu S4 genome, these genes correspond to locus tags FTT\_0354, FTT\_0378c, and FTT\_1263c. A protein databank search of this sequence also showed that it harbors 54% sequence similarity, although only 11% query cover, to the glycosyltransferase domain (GTD) of the *Clostridium difficile* toxin A (TcdA). Upon binding of the TcdA toxin to host cells, the GTD portion of the toxin is released and acts upon Rho GTPases in the cytoplasm to inactivate them via glycosylation, which triggers downstream cytopathic and cytotoxic effects (Di Bella et al., 2016). It is possible this domain may serve a similar function in the pathogenesis of *Francisella*. A previous study identified up to four homologs of this protein in *F. tularensis* and

*F. holarctica* strains, while *F. novicida* lacked a homolog of this glycosyltransferase (Barabote et al., 2009). More recently, Nau et al. (2019) demonstrated that a homolog of this transglycosylase in LVS, designated GdcA, was able to inhibit NF- $\kappa$ B signaling in immune cells.

### Phenotypic Differences Observed in the *F. tularensis* Panel

Growth of the strains in our *F. tularensis* panel was assessed in both the nutrient deplete BHI supplemented with 1% Isovitalex or the nutrient replete CDM. Interestingly, both Schu S4 strains (FRAN244 and FRAN249) grew significantly better in BHI than the other *F. tularensis* strains tested. The exact reason for enhanced growth of the Schu S4 in supplemented BHI as compared to the other strains tested here remains to be determined. Previous work showed that growth of *Francisella* in BHI broth elicited protein expression profiles similar to that of *Francisella* grown in macrophages, whereas growth in CDM and Mueller Hinton broth yielded different profiles (Hazlett et al., 2008; Holland et al., 2017). Therefore, growth differences between strains in BHI could indicate growth defects in macrophages. However, all of these strains replicated similarly in macrophages, except for FRAN037 that was decreased in CFU recovery, although not significant. Interestingly, this strain was the only one in our panel to show a growth defect in the nutrient replete CDM. It is possible the mutated FPI genes in FRAN037 contribute to this phenotype though further investigation is needed.

We also examined the LPS and capsule profiles of the panel strains using monoclonal antibodies directed against the O-antigens of these respective structures. In general when using these antibodies for characterization, no differences in the profiles were noted between the strains other than intensity differences in the banding pattern for FRAN255 at the higher molecular weight range for both the LPS and capsule. However, this does not rule out other possible differences in the LPS between strains with additional characterization. From the genomic analysis, several of the genes mutated in the *F. tularensis* panel are involved in LPS biosynthesis and transport. For example, FRAN254 contains a frameshift within the *lpxL2* gene, encoding the lipid A lauryoyltransferase. The closest relative of LpxL2 is LpxM from *Acinetobacter baumannii* (Dovala et al., 2016). LpxL and LpxM are known to share significant sequence homology and functional similarity (Six et al., 2008). In the *E. coli* LPS biosynthesis pathway, LpxL catalyzes the transfer of laurate to the Kdo<sub>2</sub>-lipid IV<sub>A</sub>, which then becomes the substrate for myristoylation by LpxM, the final enzyme in the pathway (Six et al., 2008). It has been demonstrated that deletion of *lpxL* and *lpxM* homologs in *Neisseria meningitidis* affects the resultant structure of the LPS as well as its toxicity and adjuvant activity (van der Ley et al., 2001). Interestingly, an additional *lpxL* gene encoding a smaller variant of 299 amino acids was found to be identical among all strains in our panel, indicating potential redundancy of function. These LpxL variants in *Francisella* have been previously characterized, and *lpxL* was shown to be necessary for LPS acylation, while

deletion of *lpxL2* did not appear to affect the lipid A species produced (McLendon et al., 2007).

In addition to the *lpxL* mutation, we found two mutations in *lpt* genes of two panel strains. The Lpt complex is a superstructure made of the proteins LptA-LptG and is required for LPS transport across the bacterial membrane (Wu et al., 2006). FRAN256 contained a mutation in *lptA* and FRAN255 was found to have multiple mutations in *lptD*. In *E. coli*, LptA functions to bind and transport LPS across the periplasm to the outer membrane (Schultz et al., 2017), although this protein is not well-studied in *Francisella*. The mutation identified in FRAN256 results in a frameshift and truncated protein product of 139 amino acids, in contrast to the full-length 277 amino acid variant. While no obvious LPS or capsule defect was observed in whole cell extracts of FRAN256 in this study, further investigation is required to determine if there are any subtle defects we were not able to detect by the methods employed here. The *lptD* gene, also known as *ostA*, encoding for the organic solvent tolerance protein, has two variants in *Francisella*- *ostA1* and *ostA2*. A previous study showed that deletion of *ostA2* in *F. novicida* resulted in the inability to attach and form biofilms compared to the wild-type strain (Margolis et al., 2010). This gene corresponds to *ostA2*, as evidenced by its location in the genome and sequence similarity, although it has unique features compared to the *lptD* gene from the type A isolates, including a deletion of the first 522 bp, a 3 bp in-frame deletion toward the middle of the gene, and a 180 bp extension at the end of the gene. Perhaps the slight variation observed at the higher molecular weight range of the LPS and capsule profile for FRAN255 could be contributable to this alteration for the *lptD* gene.

## Future Studies With the *F. tularensis* Challenge Panel

We are further developing this challenge panel to confirm the protective efficacy of future vaccines against pneumonic tularemia using an array of diverse *F. tularensis* strains beyond the prototype Schu S4. Due to the loss of the duplicated FPI of FRAN031 and the attenuation of FRAN037, these two strains have been eliminated from the panel and additional *F. tularensis* strains are being explored for inclusion. Preferential consideration is being given to type B strains to expand their representation as part of the panel. In addition, a recent publication has further characterized the MA00-2987 strain, a type A strain isolated from a human in 2000 from Massachusetts, U.S. in the Fischer 344 rat model (Lovchik et al., 2021). We are currently considering the addition of this strain to the panel for future testing.

Indeed, the strains making up this panel will be evolving as additional *F. tularensis* isolates of interest become available to our collection. For the strains already included in the panel, we have produced well-characterized challenge material and begun to assess virulence of these strains in a rat model of inhalational tularemia, a more appropriate challenge model for identifying virulence differences. The current *F. tularensis* panel and the Fischer rat inhalational tularemia model provides a framework

to begin to assess the efficacy of vaccine candidates against a variety of strains beyond the prototypical Schu S4 strain. For those vaccine candidates shown to be protective in the rat model, they could be transitioned for additional efficacy testing in the non-human primate pneumonic tularemia challenge model.

## DATA AVAILABILITY STATEMENT

The datasets presented in this study can be found in online repositories. The names of the repository/repositories and accession number(s) can be found in the article/**Supplementary Material**.

## ETHICS STATEMENT

The animal study was reviewed and approved by The United States Army of Medical Research Institute of Infectious Diseases Institutional Animal Care and Use Committee (USAMRIID IACUC).

## AUTHOR CONTRIBUTIONS

BB, JR, KM, DR, and JB contributed conception and design of the study and wrote the manuscript. BB, JR, KM, CK, RT, AL, KC, JS, AR, CC, DR, and JB participated in the experimentation and acquisition of data. BB, JR, KM, DF, DR, and JB were involved in the analysis or interpretation of data for the work. All the authors contributed to manuscript revision, read and approved the submitted version.

## FUNDING

This research was performed while BB and KM held a National Research Council Research Associate fellowship award supported by the CBD Research Associateship program sponsored by Defense Threat Reduction Agency. The research described herein was sponsored by the DTRA JSTO-CBD (project # CB10477).

## ACKNOWLEDGMENTS

The authors thank Tara Kenny with macrophage preparation, Michael Apicella (University of Iowa, Iowa City, IA, United States) for generously providing the monoclonal antibody 11B7, and Maureen Sullivan of the Minnesota Department of Health for providing clinical and environmental *F. tularensis* strains.

## SUPPLEMENTARY MATERIAL

The Supplementary Material for this article can be found online at: <https://www.frontiersin.org/articles/10.3389/fmicb.2021.725776/full#supplementary-material>

## REFERENCES

- Afgan, E., Baker, D., Batut, B., van den Beek, M., Bouvier, D., Čech, M., et al. (2018). The galaxy platform for accessible, reproducible and collaborative biomedical analyses: 2018 update. *Nucleic Acids Res.* 46, W537–W544. doi: 10.1093/nar/ky379
- Apicella, M. A., Post, D. M., Fowler, A. C., Jones, B. D., Rasmussen, J. A., Hunt, J. R., et al. (2010). Identification, characterization and immunogenicity of an O-antigen capsular polysaccharide of *Francisella tularensis*. *PLoS One* 5:e11060. doi: 10.1371/journal.pone.0011060
- Bachert, B. A., Biryukov, S. S., Chua, J., Rodriguez, S. A., Toothman, R. G. Jr., Cote, C. K., et al. (2019). A *Francisella novicida* mutant, lacking the soluble lytic transglycosylase Slt, exhibits defects in both growth and virulence. *Front. Microbiol.* 10:1343. doi: 10.3389/fmicb.2019.01343
- Bankevich, A., Nurk, S., Antipov, D., Gurevich, A. A., Dvorkin, M., Kulikov, A. S., et al. (2012). SPAdes: a new genome assembly algorithm and its applications to single-cell sequencing. *J. Comput. Biol.* 19, 455–477. doi: 10.1089/cmb.2012.0021
- Barabote, R. D., Xie, G., Brettin, T. S., Hinrichs, S. H., Fey, P. D., Jay, J. J., et al. (2009). Complete genome sequence of *Francisella tularensis* subspecies holarctica FTNF002-00. *PLoS One* 4:e7041. doi: 10.1371/journal.pone.0007041
- Beckstrom-Sternberg, S. M., Auerbach, R. K., Godbole, S., Pearson, J. V., Beckstrom-Sternberg, J. S., Deng, Z., et al. (2007). Complete genomic characterization of a pathogenic A.II strain of *Francisella tularensis* subspecies tularensis. *PLoS One* 2:e947. doi: 10.1371/journal.pone.0000947
- Biot, F. V., Bachert, B. A., Mlynek, K. D., Toothman, R. G., Koroleva, G. I., Lovett, S. P., et al. (2020). Evolution of antibiotic resistance in surrogates of *Francisella tularensis* (LVS and *Francisella novicida*): effects on biofilm formation and fitness. *Front. Microbiol.* 11:593542. doi: 10.3389/fmicb.2020.593542
- Bolger, A. M., Lohse, M., and Usadel, B. (2014). Trimmomatic: a flexible trimmer for Illumina sequence data. *Bioinformatics* 30, 2114–2120. doi: 10.1093/bioinformatics/btu170
- Bröms, J. E., Sjöstedt, A., and Lavander, M. (2010). The role of the *Francisella tularensis* pathogenicity island in type VI secretion, intracellular survival, and modulation of host cell signaling. *Front. Microbiol.* 1:136. doi: 10.3389/fmicb.2010.00136
- Buchele, L., and Downs, C. M. (1949). Studies on pathogenesis and immunity in tularemia; immune response of the white rat to *Bacterium tularensis*. *J. Immunol.* 63, 135–145.
- Chamberlain, R. E. (1965). Evaluation of live tularemia vaccine prepared in a chemically defined medium. *Appl. Microbiol.* 13, 232–235. doi: 10.1128/aem.13.2.232-235.1965
- Chance, T., Chua, J., Toothman, R. G., Ladner, J. T., Nuss, J. E., Raymond, J. L., et al. (2017). A spontaneous mutation in *kdsD*, a biosynthesis gene for 3 Deoxy-D-manno-Octulosonic Acid, occurred in a ciprofloxacin resistant strain of *Francisella tularensis* and caused a high level of attenuation in murine models of tularemia. *PLoS One* 12:e0174106. doi: 10.1371/journal.pone.0174106
- Chen, W., Kuolee, R., Austin, J. W., Shen, H., Che, Y., and Conlan, J. W. (2005). Low dose aerosol infection of mice with virulent type A *Francisella tularensis* induces severe thymus atrophy and CD4+CD8+ thymocyte depletion. *Microb. Pathog.* 39, 189–196. doi: 10.1016/j.micpath.2005.08.005
- Chin, C. S., Alexander, D. H., Marks, P., Klammer, A. A., Drake, J., Heiner, C., et al. (2013). Nonhybrid, finished microbial genome assemblies from long-read SMRT sequencing data. *Nat. Methods* 10, 563–569. doi: 10.1038/nmeth.2474
- Chu, P., Cunningham, A. L., Yu, J.-J., Nguyen, J. Q., Barker, J. R., Lyons, C. R., et al. (2014). Live attenuated *Francisella novicida* vaccine protects against *Francisella tularensis* pulmonary challenge in rats and non-human primates. *PLoS Pathog.* 10:e1004439. doi: 10.1371/journal.ppat.1004439
- Conlan, J. W., Chen, W., Shen, H., Webb, A., and Kuolee, R. (2003). Experimental tularemia in mice challenged by aerosol or intradermally with virulent strains of *Francisella tularensis*: bacteriologic and histopathologic studies. *Microb. Pathog.* 34, 239–248. doi: 10.1016/s0882-4010(03)00046-9
- Conlan, J. W., Shen, H., Golovliov, I., Zingmark, C., Oyston, P. C. F., Chen, W., et al. (2010). Differential ability of novel attenuated targeted deletion mutants of *Francisella tularensis* subspecies tularensis strain SCHU S4 to protect mice against aerosol challenge with virulent bacteria: Effects of host background and route of immunization. *Vaccine* 28, 1824–1831. doi: 10.1016/j.vaccine.2009.12.001
- Conway, J. R., Lex, A., and Gehlenborg, N. (2017). UpSetR: an R package for the visualization of intersecting sets and their properties. *Bioinformatics* 33, 2938–2940. doi: 10.1093/bioinformatics/btx364
- Darling, A. E., Mau, B., and Perna, N. T. (2010). progressiveMauve: multiple genome alignment with gene gain, loss and rearrangement. *PLoS One* 5:e11147. doi: 10.1371/journal.pone.0011147
- de Bruin, O. M., Duplantis, B. N., Ludu, J. S., Hare, R. F., Nix, E. B., Schmerk, C. L., et al. (2011). The biochemical properties of the *Francisella* Pathogenicity Island (FPI)-encoded proteins IglA, IglB, IglC, PdpB and DotU suggest roles in type VI secretion. *Microbiology* 157, 3483–3491. doi: 10.1099/mic.0.052308-0
- de Bruin, O. M., Ludu, J. S., and Nano, F. E. (2007). The *Francisella* pathogenicity island protein IglA localizes to the bacterial cytoplasm and is needed for intracellular growth. *BMC Microbiol.* 7:1. doi: 10.1186/1471-2180-7-1
- Dennis, D. T., Inglesby, T. V., Henderson, D. A., Bartlett, J. G., Ascher, M. S., Eitzen, E., et al. (2001). Tularemia as a biological weapon: medical and public health management. *JAMA* 285, 2763–2773. doi: 10.1001/jama.285.21.2763
- Di Bella, S., Ascenzi, P., Siarakas, S., Petrosillo, N., and di Masi, A. (2016). Clostridium difficile toxins A and B: insights into pathogenic properties and extraintestinal effects. *Toxins (Basel)* 8:134. doi: 10.3390/toxins8050134
- Dovala, D., Rath, C. M., Hu, Q., Sawyer, W. S., Shia, S., Elling, R. A., et al. (2016). Structure-guided enzymology of the lipid A acyltransferase LpxM reveals a dual activity mechanism. *Proc. Natl. Acad. Sci. U S A.* 113, E6064–E6071. doi: 10.1073/pnas.1610746113
- Downs, C. M., Coriell, L. L., Chapman, S. S., and Klauber, A. (1947a). The cultivation of *Bacterium tularensis* in embryonated eggs. *J. Bacteriol.* 53, 89–100. doi: 10.1128/jb.53.1.89-100.1947
- Downs, C. M., Coriell, L. L., Pinchot, G. B., Maumenee, E., Klauber, Alice, et al. (1947b). Studies on tularemia. I. The comparative susceptibility of various laboratory animals. *J. Immunol.* 56, 217–228.
- Downs, C. M., and Woodward, J. M. (1949). Studies on pathogenesis and immunity in tularemia; immunogenic properties for the white mouse of various strains of *Bacterium tularensis*. *J. Immunol.* 63, 147–163.
- Drabner, B., and Guzman, C. A. (2001). Elicitation of predictable immune responses by using live bacterial vectors. *Biomol. Eng.* 17, 75–82. doi: 10.1016/s1389-0344(00)00072-1
- Eigelsbach, H. T., Braun, W., and Herring, R. D. (1951). Studies on the variation of *Bacterium tularensis*. *J. Bacteriol.* 61, 557–569. doi: 10.1128/jb.61.5.557-569.1951
- Eigelsbach, H. T., and Downs, C. M. (1961). Prophylactic effectiveness of live and killed tularemia vaccines. I. Production of vaccine and evaluation in the white mouse and guinea pig. *J. Immunol.* 87, 415–425.
- Ellis, J., Oyston, P. C., Green, M., and Titball, R. W. (2002). Tularemia. *Clin. Microbiol. Rev.* 15, 631–646.
- Evans, M. E., Gregory, D. W., Schaffner, W., and McGee, Z. A. (1985). Tularemia: a 30-year experience with 88 cases. *Medicine (Baltimore)* 64, 251–269. doi: 10.1097/00005792-198507000-00006
- Farlow, J., Wagner, D. M., Dukerich, M., Stanley, M., Chu, M., Kubota, K., et al. (2005). *Francisella tularensis* in the United States. *Emerg. Infect. Dis.* 11, 1835–1841. doi: 10.3201/eid1112.050728
- Fritz, D. L., England, M. J., Miller, L., and Waag, D. M. (2014). Mouse models of aerosol-acquired tularemia caused by *Francisella tularensis* types A and B. *Comp. Med.* 64, 341–350.
- Glynn, A. R., Alves, D. A., Frick, O., Erwin-Cohen, R., Porter, A., Norris, S., et al. (2015). Comparison of experimental respiratory tularemia in three nonhuman primate species. *Comp. Immunol. Microbiol. Infect. Dis.* 39, 13–24. doi: 10.1016/j.cimid.2015.01.003
- Goethert, H. K., Shani, I., and Telford, S. R. III (2004). Genotypic diversity of *Francisella tularensis* infecting Dermacentor variabilis ticks on Martha's Vineyard, Massachusetts. *J. Clin. Microbiol.* 42, 4968–4973. doi: 10.1128/JCM.42.11.4968-4973.2004
- Golovliov, I., Twine, S. M., Shen, H., Sjöstedt, A., and Conlan, W. (2013). A DeltaclpB mutant of *Francisella tularensis* subspecies holarctica strain, FSC200,

- is a more effective live vaccine than *F. tularensis* LVS in a mouse respiratory challenge model of tularemia. *PLoS One* 8:e78671. doi: 10.1371/journal.pone.0078671
- Goris, J., Konstantinidis, K. T., Klappenbach, J. A., Coenye, T., Vandamme, P., and Tiedje, J. M. (2007). DNA–DNA hybridization values and their relationship to whole-genome sequence similarities. *Int. J. Syst. Evol. Microbiol.* 57, 81–91. doi: 10.1099/ijs.0.64483-0
- Guina, T., Lanning, L. L., Omland, K. S., Williams, M. S., Wolfrain, L. A., Heyse, S. P., et al. (2018). The cynomolgus macaque natural history model of pneumonic tularemia for predicting clinical efficacy under the animal rule. *Front. Cell. Infect. Microbiol.* 8:99. doi: 10.3389/fcimb.2018.0099
- Hadfield, J., Croucher, N. J., Goater, R. J., Abudahab, K., Aanensen, D. M., and Harris, S. R. (2017). Phandango: an interactive viewer for bacterial population genomics. *Bioinformatics* 34, 292–293. doi: 10.1093/bioinformatics/btx610
- Harris, S. (1992). Japanese biological warfare research on humans: a case study of microbiology and ethics. *Ann. N. Y. Acad. Sci.* 666, 21–52. doi: 10.1111/j.1749-6632.1992.tb38021.x
- Hazlett, K. R., Caldon, S. D., McArthur, D. G., Cirillo, K. A., Kirimanjeswara, G. S., Magguilli, M. L., et al. (2008). Adaptation of *Francisella tularensis* to the mammalian environment is governed by cues which can be mimicked in vitro. *Infect. Immun.* 76, 4479–4488. doi: 10.1128/iai.00610-08
- Heine, H. S., Chuvala, L., Riggins, R., Cirz, R., Cass, R., Louie, A., et al. (2016). Natural history of *Francisella tularensis* in aerosol-challenged BALB/c mice. *Antimicrob. Agents Chemother.* 60, 1834–1840. doi: 10.1128/AAC.02887-15
- Hesselbrock, W., and Foshay, L. (1945). The morphology of bacterium tularensis. *J. Bacteriol.* 49, 209–231. doi: 10.1128/jb.49.3.209-231.1945
- Holland, K. M., Rosa, S. J., Kristjansdottir, K., Wolfgeher, D., Franz, B. J., Zarrella, T. M., et al. (2017). Differential growth of *Francisella tularensis*, which alters expression of virulence factors, dominant antigens, and surface-carbohydrate synthases, governs the apparent virulence of Ft SchuS4 to immunized animals. *Front. Microbiol.* 8:1158. doi: 10.3389/fmicb.2017.01158
- Hutt, J. A., Lovchik, J. A., Dekonenko, A., Hahn, A. C., and Wu, T. H. (2017). The natural history of pneumonic tularemia in female Fischer 344 rats after inhalational exposure to aerosolized *Francisella tularensis* subspecies tularensis strain SCHU S4. *Am. J. Pathol.* 187, 252–267. doi: 10.1016/j.ajpath.2016.09.021
- Jellison, W. L. (1950). Tularemia; geographical distribution of deerfly fever and the biting fly, *Chrysops discalis* Williston. *Public Health Rep.* 65, 1321–1329.
- Jemski, J. V. (1981). Respiratory tularemia: comparison of selected routes of vaccination in Fischer 344 rats. *Infect. Immun.* 34, 766–772. doi: 10.1128/iai.34.3.766-772.1981
- Jia, Q., Bowen, R., Dillon, B. J., Maslesa-Galic, S., Chang, B. T., Kaidi, A. C., et al. (2018). Single vector platform vaccine protects against lethal respiratory challenge with Tier 1 select agents of anthrax, plague, and tularemia. *Sci. Rep.* 8:7009. doi: 10.1038/s41598-018-24581-y
- Jia, Q., Bowen, R., Lee, B. Y., Dillon, B. J., Maslesa-Galić, S., and Horwitz, M. A. (2016). *Francisella tularensis* Live vaccine strain deficient in capB and overexpressing the fusion protein of IglA, IglB, and IglC from the bfr promoter induces improved protection against *F. tularensis* respiratory challenge. *Vaccine* 34, 4969–4978. doi: 10.1016/j.vaccine.2016.08.041
- Jia, Q., Bowen, R., Sahakian, J., Dillon, B. J., and Horwitz, M. A. (2013). A heterologous prime-boost vaccination strategy comprising the *Francisella tularensis* live vaccine strain capB mutant and recombinant attenuated *Listeria monocytogenes* expressing *F. tularensis* IglC induces potent protective immunity in mice against virulent *F. tularensis* aerosol challenge. *Infect. Immun.* 81, 1550–1561. doi: 10.1128/iai.01013-12
- Jia, Q., and Horwitz, M. A. (2018). Live attenuated tularemia vaccines for protection against respiratory challenge with virulent *F. tularensis* subsp. tularensis. *Front. Cell. Infect. Microbiol.* 8:154. doi: 10.3389/fcimb.2018.00154
- Jia, Q., Lee, B. Y., Bowen, R., Dillon, B. J., Som, S. M., and Horwitz, M. A. (2010). A *Francisella tularensis* live vaccine strain (LVS) mutant with a deletion in capB, encoding a putative capsular biosynthesis protein, is significantly more attenuated than LVS yet induces potent protective immunity in mice against *F. tularensis* challenge. *Infect. Immun.* 78, 4341–4355. doi: 10.1128/iai.00192-10
- Johnson, S. L., Daligault, H. E., Davenport, K. W., Coyne, S. R., Frey, K. G., Koroleva, G. I., et al. (2015). Genome sequencing of 18 francisella strains to aid in assay development and testing. *Genome Announc.* 3:e00147–15. doi: 10.1128/genomeA.00147-15
- Jones, B. D., Faron, M., Rasmussen, J. A., and Fletcher, J. R. (2014). Uncovering the components of the *Francisella tularensis* virulence stealth strategy. *Front. Cell. Infect. Microbiol.* 4:32. doi: 10.3389/fcimb.2014.00032
- Kanistanon, D., Hajjar, A. M., Pelletier, M. R., Gallagher, L. A., Kalthorn, T., Shaffer, S. A., et al. (2008). A *Francisella* mutant in lipid A carbohydrate modification elicits protective immunity. *PLoS Pathog.* 4:e24. doi: 10.1371/journal.ppat.0040024
- Kijek, T. M., Mou, S., Bachert, B. A., Kuehl, K. A., Williams, J. A., Daye, S. P., et al. (2019). The D-alanyl-d-alanine carboxypeptidase enzyme is essential for virulence in the Schu S4 strain of *Francisella tularensis* and a daeD mutant is able to provide protection against a pneumonic challenge. *Microb. Pathog.* 137:103742. doi: 10.1016/j.micpath.2019.103742
- Kim, T. H., Pinkham, J. T., Heninger, S. J., Chalabaev, S., and Kasper, D. L. (2012). Genetic modification of the O-polysaccharide of *Francisella tularensis* results in an avirulent live attenuated vaccine. *J. Infect. Dis.* 205, 1056–1065. doi: 10.1093/infdis/jir620
- Kolmogorov, M., Yuan, J., Lin, Y., and Pevzner, P. A. (2019). Assembly of long, error-prone reads using repeat graphs. *Nat. Biotechnol.* 37, 540–546. doi: 10.1038/s41587-019-0072-8
- Kugeler, K. J., Mead, P. S., Janusz, A. M., Staples, J. E., Kubota, K. A., Chalcraft, L. G., et al. (2009). Molecular epidemiology of *Francisella tularensis* in the United States. *Clin. Infect. Dis.* 48, 863–870. doi: 10.1086/597261
- Kumar, R., Bröms, J. E., and Sjöstedt, A. (2020). Exploring the diversity within the genus *Francisella* - an integrated pan-genome and genome-mining approach. *Front. Microbiol.* 11:1928. doi: 10.3389/fmicb.2020.01928
- Larsson, P., Elfsmark, D., Svensson, K., Wikström, P., Forsman, M., Brettin, T., et al. (2009). Molecular evolutionary consequences of niche restriction in *Francisella tularensis*, a facultative intracellular pathogen. *PLoS Pathog.* 5:e1000472. doi: 10.1371/journal.ppat.1000472
- Larsson, P., Oyston, P. C., Chain, P., Chu, M. C., Duffield, M., Fuxelius, H. H., et al. (2005). The complete genome sequence of *Francisella tularensis*, the causative agent of tularemia. *Nat. Genet.* 37, 153–159. doi: 10.1038/ng1499
- Li, H. (2018). Minimap2: pairwise alignment for nucleotide sequences. *Bioinformatics* 34, 3094–3100. doi: 10.1093/bioinformatics/bty191
- Lindgren, M., Eneslätt, K., Bröms, J. E., and Sjöstedt, A. (2013). Importance of PdpC, IglC, IglI, and IglG for modulation of a host cell death pathway induced by *Francisella tularensis*. *Infect. Immun.* 81, 2076–2084. doi: 10.1128/iai.00275-13
- Lovchik, J. A., Reed, D. S., Hutt, J. A., Xia, F., Stevens, R. L., Modise, T., et al. (2021). Identification of an attenuated substrain of *Francisella tularensis* SCHU S4 by phenotypic and genotypic analyses. *Pathogens* 10:638. doi: 10.3390/pathogens10060638
- Mansour, A. A., Banik, S., Suresh, R. V., Kaur, H., Malik, M., McCormick, A. A., et al. (2018). An improved Tobacco Mosaic Virus (TMV)-conjugated multiantigen subunit vaccine against respiratory tularemia. *Front. Microbiol.* 9:1195. doi: 10.3389/fmicb.2018.01195
- Margolis, J. J., El-Etr, S., Joubert, L. M., Moore, E., Robison, R., Rasley, A., et al. (2010). Contributions of *Francisella tularensis* subsp. novicida chitinases and Sec secretion system to biofilm formation on chitin. *Appl. Environ. Microbiol.* 76, 596–608. doi: 10.1128/aem.02037-09
- Markowitz, L. E., Hynes, N. A., de la Cruz, P., Campos, E., Barbaree, J. M., Plikaytis, B. D., et al. (1985). Tick-borne tularemia. An outbreak of lymphadenopathy in children. *JAMA* 254, 2922–2925. doi: 10.1001/jama.1985.03360200074030
- Marshall, L. E., Nelson, M., Davies, C. H., Whelan, A. O., Jenner, D. C., Moule, M. G., et al. (2018). An O-antigen glycoconjugate vaccine produced using protein glycan coupling technology is protective in an inhalational rat model of tularemia. *J. Immunol. Res.* 2018:8087916. doi: 10.1155/2018/8087916
- McCrumb, F. R. (1961). Aerosol infection of man with *Pasteurella tularensis*. *Bacteriol. Rev.* 25, 262–267. doi: 10.1128/membr.25.3.262-267.1961

- McLendon, M. K., Schilling, B., Hunt, J. R., Apicella, M. A., and Gibson, B. W. (2007). Identification of LpxL, a late acyltransferase of *Francisella tularensis*. *Infect. Immun.* 75, 5518–5531. doi: 10.1128/iai.01288-06
- Molins, C. R., Delorey, M. J., Yockey, B. M., Young, J. W., Belisle, J. T., Schriefer, M. E., et al. (2014). Virulence difference between the prototypic Schu S4 strain (A1a) and *Francisella tularensis* A1a, A1b, A2 and type B strains in a murine model of infection. *BMC Infect. Dis.* 14:67. doi: 10.1186/1471-2334-14-67
- Moran, N. A., and Plague, G. R. (2004). Genomic changes following host restriction in bacteria. *Curr. Opin. Genet. Dev.* 14, 627–633. doi: 10.1016/j.gde.2004.09.003
- Nano, F. E., and Schmerk, C. (2007). The Francisella pathogenicity island. *Ann. N. Y. Acad. Sci.* 1105, 122–137. doi: 10.1196/annals.1409.000
- Nano, F. E., Zhang, N., Cowley, S. C., Klose, K. E., Cheung, K. K., Roberts, M. J., et al. (2004). A *Francisella tularensis* pathogenicity island required for intramacrophage growth. *J. Bacteriol.* 186, 6430–6436. doi: 10.1128/JB.186.19.6430-6436.2004
- Nau, G. J., Horzempa, J., O'Dee, D., Brown, M. J., Russo, B. C., Hernandez, A., et al. (2019). A predicted *Francisella tularensis* DXD-motif glycosyltransferase blocks immune activation. *Virulence* 10, 643–656. doi: 10.1080/21505594.2019.1631662
- Okonechnikov, K., Golosova, O., and Fursov, M. (2012). Unipro UGENE: a unified bioinformatics toolkit. *Bioinformatics* 28, 1166–1167. doi: 10.1093/bioinformatics/bts091
- Page, A. J., Cummins, C. A., Hunt, M., Wong, V. K., Reuter, S., Holden, M. T. G., et al. (2015). Roary: rapid large-scale prokaryote pan genome analysis. *Bioinformatics* 31, 3691–3693. doi: 10.1093/bioinformatics/btv421
- Pandya, G. A., Holmes, M. H., Petersen, J. M., Pradhan, S., Karamycheva, S. A., Wolcott, M. J., et al. (2009). Whole genome single nucleotide polymorphism based phylogeny of *Francisella tularensis* and its application to the development of a strain typing assay. *BMC Microbiol.* 9:213. doi: 10.1186/1471-2180-9-213
- Pechous, R. D., McCarthy, T. R., Mohapatra, N. P., Soni, S., Penoske, R. M., Salzman, N. H., et al. (2008). A *Francisella tularensis* Schu S4 purine auxotroph is highly attenuated in mice but offers limited protection against homologous intranasal challenge. *PLoS One* 3:e2487. doi: 10.1371/journal.pone.0002487
- Post, D. M. B., Slütter, B., Schilling, B., Chande, A. T., Rasmussen, J. A., Jones, B. D., et al. (2017). Characterization of inner and outer membrane proteins from *Francisella tularensis* strains LVS and Schu S4 and identification of potential subunit vaccine candidates. *mBio* 8:e01592–17. doi: 10.1128/mBio.01592-17
- Rasmussen, J. A., Fletcher, J. R., Long, M. E., Allen, L. A., and Jones, B. D. (2015). Characterization of *Francisella tularensis* Schu S4 mutants identified from a transposon library screened for O-antigen and capsule deficiencies. *Front. Microbiol.* 6:338. doi: 10.3389/fmicb.2015.00338
- Rasmussen, J. A., Post, D. M., Gibson, B. W., Lindemann, S. R., Apicella, M. A., Meyerholz, D. K., et al. (2014). *Francisella tularensis* Schu S4 lipopolysaccharide core sugar and O-antigen mutants are attenuated in a mouse model of tularemia. *Infect. Immun.* 82, 1523–1539. doi: 10.1128/IAI.01640-13
- Ray, H. J., Chu, P., Wu, T. H., Lyons, C. R., Murthy, A. K., Guentzel, M. N., et al. (2010). The Fischer 344 rat reflects human susceptibility to Francisella pulmonary challenge and provides a new platform for virulence and protection studies. *PLoS One* 5:e9952. doi: 10.1371/journal.pone.0009952
- Raynaud, C., Meibom, K. L., Lety, M. A., Dubail, I., Candela, T., Frapy, E., et al. (2007). Role of the wbt locus of *Francisella tularensis* in lipopolysaccharide O-antigen biogenesis and pathogenicity. *Infect. Immun.* 75, 536–541. doi: 10.1128/IAI.01429-06
- Rodriguez-R, L. M., and Konstantinidis, K. T. (2016). The enveomics collection: a toolbox for specialized analyses of microbial genomes and metagenomes. *PeerJ Preprints* 4:e1900v1901. doi: 10.7287/peerj.preprints.1900v1
- Rohmer, L., Brittnacher, M., Svensson, K., Buckley, D., Haugen, E., Zhou, Y., et al. (2006). Potential source of *Francisella tularensis* live vaccine strain attenuation determined by genome comparison. *Infect. Immun.* 74, 6895–6906. doi: 10.1128/iai.01006-06
- Russo, B. C., Horzempa, J., O'Dee, D. M., Schmitt, D. M., Brown, M. J., Carlson, P. E. Jr., et al. (2011). A *Francisella tularensis* locus required for spermine responsiveness is necessary for virulence. *Infect. Immun.* 79, 3665–3676. doi: 10.1128/IAI.00135-11
- Sandstrom, G., Sjostedt, A., Johansson, T., Kuoppa, K., and Williams, J. C. (1992). Immunogenicity and toxicity of lipopolysaccharide from *Francisella tularensis* LVS. *FEMS Microbiol. Immunol.* 5, 201–210. doi: 10.1111/j.1574-6968.1992.tb05902.x
- Saslaw, S., Eigelsbach, H. T., Prior, J. A., Wilson, H. E., and Carhart, S. (1961a). Tularemia vaccine study. II. Respiratory challenge. *Arch. Intern. Med.* 107, 702–714. doi: 10.1001/archinte.1961.03620050068007
- Saslaw, S., Eigelsbach, H. T., Wilson, H. E., Prior, J. A., and Carhart, S. (1961b). Tularemia vaccine study. I. Intracutaneous challenge. *Arch. Intern. Med.* 107, 689–701. doi: 10.1001/archinte.1961.03620050055006
- Schmerk, C. L., Duplantis, B. N., Howard, P. L., and Nano, F. E. (2009a). A *Francisella novicida* pdpA mutant exhibits limited intracellular replication and remains associated with the lysosomal marker LAMP-1. *Microbiology* 155, 1498–1504. doi: 10.1099/mic.0.025445-0
- Schmerk, C. L., Duplantis, B. N., Wang, D., Burke, R. D., Chou, A. Y., Elkins, K. L., et al. (2009b). Characterization of the pathogenicity island protein PdpA and its role in the virulence of *Francisella novicida*. *Microbiology* 155, 1489–1497. doi: 10.1099/mic.0.025379-0
- Schultz, K. M., Lundquist, T. J., and Klug, C. S. (2017). Lipopolysaccharide binding to the periplasmic protein LptA. *Protein Sci.* 26, 1517–1523. doi: 10.1002/pro.3177
- Seemann, T. (2014). Prokka: rapid prokaryotic genome annotation. *Bioinformatics* 30, 2068–2069. doi: 10.1093/bioinformatics/btu153
- Six, D. A., Carty, S. M., Guan, Z., and Raetz, C. R. (2008). Purification and mutagenesis of LpxL, the lauroyltransferase of *Escherichia coli* lipid A biosynthesis. *Biochemistry* 47, 8623–8637. doi: 10.1021/bi800873n
- Snipen, L., and Liland, K. H. (2015). micropan: an R-package for microbial pan-genomics. *BMC Bioinform.* 16:79. doi: 10.1186/s12859-015-0517-0
- Su, J., Yang, J., Zhao, D., Kawula, T. H., Banas, J. A., and Zhang, J. R. (2007). Genome-wide identification of *Francisella tularensis* virulence determinants. *Infect. Immun.* 75, 3089–3101. doi: 10.1128/IAI.01865-06
- R. C. Team. (2020). *R: A language and environment for statistical computing*. Vienna, Austria: R Foundation for Statistical Computing.
- Tempel, R., Lai, X. H., Crosa, L., Kozlowski, B., and Heffron, F. (2006). Attenuated *Francisella novicida* transposon mutants protect mice against wild-type challenge. *Infect. Immun.* 74, 5095–5105. doi: 10.1128/iai.00598-06
- Tigert, W. D. (1962). Soviet viable Pasteurella tularensis vaccines. A review of selected articles. *Bacteriol. Rev.* 26, 354–373. doi: 10.1128/membr.26.3.354-373.1962
- Twenhafel, N. A., Alves, D. A., and Purcell, B. K. (2009). Pathology of inhalational *Francisella tularensis* spp. tularensis SCHU S4 infection in African green monkeys (*Chlorocebus aethiops*). *Vet. Pathol.* 46, 698–706. doi: 10.1354/vp.08-VP-0302-T-AM
- Twine, S. M., Shen, H., Kelly, J. F., Chen, W., Sjostedt, A., and Conlan, J. W. (2006). Virulence comparison in mice of distinct isolates of type A *Francisella tularensis*. *Microb. Pathog.* 40, 133–138. doi: 10.1016/j.micpath.2005.12.004
- van der Ley, P., Steeghs, L., Hamstra, H. J., ten Hove, J., Zomer, B., and van Alphen, L. (2001). Modification of lipid A biosynthesis in *Neisseria meningitidis* lpxL mutants: influence on lipopolysaccharide structure, toxicity, and adjuvant activity. *Infect. Immun.* 69, 5981–5990. doi: 10.1128/iai.69.10.5981-5990.2001
- Van Zandt, K. E., Tuanyok, A., Keim, P. S., Warren, R. L., and Gelhaus, H. C. (2012). An objective approach for Burkholderia pseudomallei strain selection as challenge material for medical countermeasures efficacy testing. *Front. Cell. Infect. Microbiol.* 2:120. doi: 10.3389/fcimb.2012.00120
- Vogler, A. J., Birdsell, D., Price, L. B., Bowers, J. R., Beckstrom-Sternberg, S. M., Auerbach, R. K., et al. (2009). Phylogeography of *Francisella tularensis*: global expansion of a highly fit clone. *J. Bacteriol.* 191, 2474–2484. doi: 10.1128/jb.01786-08
- Walker, B. J., Abeel, T., Shea, T., Priest, M., Abouelliel, A., Sakthikumar, S., et al. (2014). Pilon: an integrated tool for comprehensive microbial variant detection and genome assembly improvement. *PLoS One* 9:e112963. doi: 10.1371/journal.pone.0112963

- Wang, X., Ribeiro, A. A., Guan, Z., Abraham, S. N., and Raetz, C. R. (2007). Attenuated virulence of a *Francisella* mutant lacking the lipid A 4'-phosphatase. *Proc. Natl. Acad. Sci. U.S.A.* 104, 4136–4141. doi: 10.1073/pnas.0611606104
- Wang, X., Ribeiro, A. A., Guan, Z., McGrath, S. C., Cotter, R. J., and Raetz, C. R. (2006). Structure and biosynthesis of free lipid A molecules that replace lipopolysaccharide in *Francisella tularensis* subsp. novicida. *Biochemistry* 45, 14427–14440. doi: 10.1021/bi061767s
- Weiss, D. S., Brotcke, A., Henry, T., Margolis, J. J., Chan, K., and Monack, D. M. (2007). In vivo negative selection screen identifies genes required for *Francisella* virulence. *Proc. Natl. Acad. Sci. U.S.A.* 104, 6037–6042. doi: 10.1073/pnas.0609675104
- Whelan, A. O., Flick-Smith, H. C., Homan, J., Shen, Z. T., Carpenter, Z., Khoshkenar, P., et al. (2018). Protection induced by a *Francisella tularensis* subunit vaccine delivered by glucan particles. *PLoS One* 13:e0200213. doi: 10.1371/journal.pone.0200213
- Wick, R. (2020). *Filtlong*. Available online at: <https://github.com/rrwick/Filtlong>; Github.
- Wick, R. R., Judd, L. M., Gorrie, C. L., and Holt, K. E. (2017). Unicycler: Resolving bacterial genome assemblies from short and long sequencing reads. *PLoS Comput. Biol.* 13:e1005595. doi: 10.1371/journal.pcbi.1005595
- Wu, T., McCandlish, A. C., Gronenberg, L. S., Chng, S. S., Silhavy, T. J., and Kahne, D. (2006). Identification of a protein complex that assembles lipopolysaccharide in the outer membrane of *Escherichia coli*. *Proc. Natl. Acad. Sci. U.S.A.* 103, 11754–11759. doi: 10.1073/pnas.0604744103
- Zweitering, M. H., Jongenburger, I., Rombouts, F. M., and Van't Riet, K. (1990). Modeling of the bacterial growth curve. *Appl. Environ. Microb.* 56, 1875–1881. doi: 10.1128/aem.56.6.1875-1881.1990
- Author Disclaimer:** Opinions, interpretations, conclusions, and recommendations are those of the authors and are not necessarily endorsed by the U.S. Army.
- Conflict of Interest:** The authors declare that the research was conducted in the absence of any commercial or financial relationships that could be construed as a potential conflict of interest.
- Publisher's Note:** All claims expressed in this article are solely those of the authors and do not necessarily represent those of their affiliated organizations, or those of the publisher, the editors and the reviewers. Any product that may be evaluated in this article, or claim that may be made by its manufacturer, is not guaranteed or endorsed by the publisher.

Copyright © 2021 Bachert, Richardson, Mlynek, Klimko, Toothman, Fetterer, Luquette, Chase, Storrs, Rogers, Cote, Rozak and Bozue. This is an open-access article distributed under the terms of the Creative Commons Attribution License (CC BY). The use, distribution or reproduction in other forums is permitted, provided the original author(s) and the copyright owner(s) are credited and that the original publication in this journal is cited, in accordance with accepted academic practice. No use, distribution or reproduction is permitted which does not comply with these terms.